Master's thesis

NTNU
Norwegian University of Science and Technology
Faculty of Natural Sciences
Department of Biology

Ingrid Gisnås Vardeberg

Disruption of Melatonin, Serotonin, and Adenosine Receptors by Chemicals in Plastic Food Packaging

Master's thesis in Biotechnology
Supervisor: Martin Wagner
Co-supervisor: Molly Y. McPartland
November 2022

NTNU
Norwegian University of
Science and Technology

Ingrid Gisnås Vardeberg

Disruption of Melatonin, Serotonin, and Adenosine Receptors by Chemicals in Plastic Food Packaging

Master's thesis in Biotechnology
Supervisor: Martin Wagner
Co-supervisor: Molly Y. McPartland
November 2022

Norwegian University of Science and Technology
Faculty of Natural Sciences
Department of Biology

NTNU
Norwegian University of
Science and Technology

Acknowledgments

This thesis, comprising 60 ECTS credits, marks the end of my MSc of Science in Biotechnology. The thesis was written at the Department of Biology, Norwegian University of Science and Technology (NTNU), Trondheim, Norway 2022. The thesis was financed through the Wagner group, NTNU, and funding provided by NTNU in association with Molly McPartland's Ph.D. project.

I want to thank Martin Wagner and Molly McPartland, my supervisors at the Department of Biology (NTNU) for all your guidance, support, and feedback during these two years. Martin, I admire your dedication to research for a better world. Not only are you a great scientist and an important voice in environmental politics, but your patience, never-ending curiosity, and inspiring leadership are just some of the qualities I truly admire. Molly, you've shown me how to reach my goals with hard work and dedication, and I'm forever grateful for everything you've taught me regarding research planning, laboratory techniques, data analysis, and writing skills. I admire your whole-hearted enthusiasm for science, and I truly appreciate your motivating pep talks and your commitment for me to reach my full potential. Thank you, both.

I wish to express gratitude to the rest of the Wagner group for all their support and feedback, and especially to Trude Johansen and Sarah Stevens for always taking the time to answer my questions and share your knowledge. Further, I'm thankful to my loving family, partner, and friends for allowing me to vent my struggles, for always cheering me on, and for believing in me through it all. Last, but certainly not least, my dear friend and fellow student in the Wagner group, Åsa Vedøy, deserves a huge thank you for your moral support and companionship ever since we first met in 2017. I wouldn't want to share this journey with anyone else.

Trondheim, November 2022,

Ingrid Gisnås Vardeberg

Abstract

Plastics are versatile materials with beneficial properties such as durability, light weight, and low price, making them suitable for a wide range of consumer products. Plastics have great societal benefits, for instance when used as food contact materials for preserving foodstuff. However, human exposure to plastic chemicals is of concern as several plastic chemicals have negative health impacts and further, as the chemicals can migrate from the packaging into the foodstuff. Since many of the substances in plastics are truly unknown, possible impacts of exposure cannot be addressed. Thus, the human health effect of plastic chemicals is of concern. Since most research on receptor signal disruption by plastic chemicals have been conducted on nuclear receptors, this study sought to provide novel insight to plastic chemical disruption of G protein-coupled receptors.

By combining cytotoxicity testing, PRESTO-Tango assays, and chemical analysis of receptor activating plastic samples, this study investigated whether agonists for G protein-coupled receptors are present in food contact articles made of five polymer types (polyethylene, polypropylene, polystyrene, polyurethane, and polyvinyl chloride). We studied five G protein-coupled receptors of therapeutical importance, including the melatonin receptors MTNR1A and MTNR1B, serotonin receptors HTR1A and HTR2C, and the adenosine receptor ADORA1. We extracted plastic chemicals from food contact articles, and then performed cytotoxicity experiments to ensure non-cytotoxic plastic exposure in the PRESTO-Tango assay. We then conducted PRESTO-Tango assays to identify individual plastic samples that contained G protein-coupled receptor agonists. Lastly, we used data from non-target chemical analysis on the activating plastic samples to narrow down the list of agonist candidates.

We concluded that polyurethane was the most cytotoxic sample, and further, that a mixture effect of the polyvinyl chloride mix was apparent. We confirmed PRESTO-Tango assays for four of the five receptors studied in this thesis (MTNR1A, MTNR1B, HTR1A, and ADORA1) by reference compounds. The chemicals present in two polyvinyl chloride samples activated MTNR1A while one polyurethane and one polyvinyl chloride sample activated ADORA1. For the active plastic samples, we greatly reduced the list of possible agonists obtained from non-target chemical analysis, and all combined, this study shows that food contact articles contain numerous potential G protein-coupled receptor agonists.

The results of this study emphasizes the importance of further research on food contact chemicals' realistic impact on human health. Challenges of mixture effects and non-intentionally added substances of plastics should be addressed, and moreover, international regulations and transparency regarding plastic production is called for to approach plastic products that do not pose a risk to human health.

Sammendrag

Plast er et allsidig materiale med fordelaktige egenskaper, som holdbarhet, lav vekt og lave priser. Dette gjør materialet egnet for et bredt spekter av forbrukerprodukter. Plast er av stor samfunnsmessig interesse, blant annet fordi materialet er avgjørende for matkonservering. Menneskelig eksponering for plastkjemikalier fra produkter som er i kontakt med mat er imidlertid bekymringsfull ettersom plastkjemikalier kan migrere fra emballasje til mat. Mange av stoffene i plast er ukjente og det er derfor ikke mulig å vite virkninger av disse. Helseeffekten av plastkjemikalier er følgelig bekymringsverdig. Siden det meste av forskning på reseptorsignalforstyrrende plastkjemikalier har blitt utført på cellekjernereseptorer, etterstreber denne studien å gi ny innsikt i plastkjemikalieforstyrrelse av G-proteinkoblede reseptorer.

Denne studien undersøker hvorvidt agonister for G-proteinkoblede reseptorer er til stede i plastprodukter laget av fem polymertyper (polyetylen, polypropylen, polystyren, polyuretan og polyvinylklorid). Dette gjøres ved å kombinere cytotoksisitetstesting, PRESTO-Tango-analyser og kjemisk analyse av reseptor-aktiverende plastekstrakter. Vi studerte fem G-proteinkoblede reseptorer av terapeutisk betydning, inkludert to melatonin-reseptorer (MTNR1A og MTNR1B), to serotonin-reseptorer (HTR1A og HTR2C) og én adenosin-reseptor (ADORA1). For å undersøke plastkjemikalieeffekten på disse reseptorene, ekstraherte vi kjemikalier fra plastprodukter brukt til matoppbevaring. Deretter utførte vi cytotoksisitetsforsøk for å sikre at toksiske konsentrasjoner av plastekstraktene ikke ble brukt i PRESTO-Tango-analysene. Så utførte vi PRESTO-Tango-analyser for å identifisere individuelle plastprøver som inneholdt agonister for G-proteinkoblede reseptorer. Til slutt brukte vi data fra non-target-analyser av de aktiverende plastekstraktene for å redusere antall agonistkandidater.

Vi konkluderer med at polyuretan er den mest cytotoksiske plastprøven, og videre at en blandingseffekt av polyvinylklorid-prøvene er tydelig. Fungerende PRESTO-Tango-analyser ble bekreftet med referanseforbindelser for fire av fem G-proteinkoblede reseptorer undersøkt i denne studien (MTNR1A, MTNR1B, HTR1A og ADORA1). Kjemikaliene i to polyvinylklorid-prøver aktiverte MTNR1A, mens én polyuretan- og én polyvinylklorid-prøve aktiverte ADORA1. Listen over mulige agonister fra de aktiverende plastekstraktene ble betraktelig redusert. Alt tatt i betraktning viser denne studien at plastprodukter i kontakt med mat inneholder mange potensielle agonister for G-proteinkoblede reseptorer.

Resultatene av denne studien understreker viktigheten av videre forskning på plastkjemikaliers faktiske innvirkning på menneskers helse. Effekten av polymerblandinger og ikke-tilsiktede substanser i plast bør undersøkes videre. I tillegg bør internasjonale reguleringer og åpenhet rundt plastproduksjon adresseres for å etablere produkter som ikke utgjør risiko for menneskehelse.

Contents

Abbreviations

5-HT	Serotonin
ADORA1	Adenosine receptor A_1
ADP	Adenosine diphosphate
AMP	Adenosine monophosphate
ATP	Adenosine triphosphate
BPA	Bisphenol A
DEHP	Di-(2-ethylhexyl) phthalates
DMSO	Dimethyl sulfoxide
E. coli	*Escherichia coli*
EC_{20}	Maximal effect concentration, 20%
EC_{50}	Maximal effect concentration, 50%
EU	European Union
FCAs	Food contact articles
FCCs	Food contact chemicals
FCMs	Food contact materials
GDP	Guanosine diphosphate
GPC30	G protein receptor 30
GPCR	G protein-coupled receptor
GPER	G protein-coupled estrogen receptor
GRKs	GPCR kinases
GTP	Guanosine triphosphate
hERα	Human estrogen receptor α
HNC	Highest non-cytotoxic concentration
HTR1A	Serotonin receptor 1A
HTR2C	Serotonin receptor 2C
LB	Lysogeny broth
LH	Luteinizing hormone
LOD	Limit of detection
LSD	Lysergic acid diethylamide
MT	Melatonin
MTNR1A	Melatonin receptor 1A
MTNR1B	Melatonin receptor 1B

NECA	5′-N-ethylcarboxamide adenosine
NIAS	Non-intentionally added substances
PB	Procedure blank
PBS	Phosphate-buffered saline
PE	Polyethylene
PLL	Poly-L-lysine
PP	Polypropylene
PPARγ	Peroxisome proliferator-activated receptor γ
PS	Polystyrene
PUR	Polyurethane
PVC	Polyvinyl chloride
SHBG	Sex hormone-binding globulin
TE	Tris-EDTA
TEV	Tobacco etch virus
tTA	Tethered transcriptional activator

1. Introduction

1.1 Plastics

Plastics have a variety of benefits including low weight, durability, toughness, and low density making it a versatile material that is ubiquitously used in our society today (Andrady and Neal, 2009). One could argue that plastic has positive environmental effects. For example, lightweight plastic used in packaging and transport results in lower fuel consumption. Moreover, plastic has insulating properties which, in electrical applications, improve the energy efficiency and thus, reduce emission of greenhouse gases (World Health Organization, 2022). From a health perspective, plastic offer a wide range of usage with direct human health benefits. For instance, plastic is being used in sterile medical equipment such as intravenous tubes, syringes, catheters, examination gloves, and bandages. The use of plastic in these devices is crucial, and the benefits of it rules out any competitive materials (Andrady and Neal, 2009). Further, plastics are of great societal interest because of their ability to preserve food by reducing soiling, physical damage, and microbial spoilage, and thus, reducing food waste (Muncke et al., 2017, World Health Organization, 2022). When plastics are used in relation to food (e.g., production, handling, or storage), they are categorized as food contact materials (FCMs) which make up the larger overall food contact articles (FCAs, Figure 1, Muncke et al., 2017).

Plastic constitutes of synthetic polymers as the main ingredient, and different polymers hold different properties that form products of varying use. Examples include polyethylene (PE) being used in containers and toys, polypropylene (PP) being used in microwave containers and snack wrappers, polystyrene (PS) being used in building insulation and electronic equipment, polyurethane (PUR) being used in pillows and insulating foams, and polyvinyl chloride (PVC) being used in pipes and garden hoses (PlasticsEurope, 2021). Further, plastic consist of different additives, that are chemical compounds which are intentionally added to the polymer to change the properties and thus application of the plastic. Common additives are plasticizers, light and heat stabilizers, flame retardants, slip agents, lubricants, pigments, antistatic agents, antioxidants, and acid scavengers. Each of these plays a specific role in how the final plastic product performs (Hahladakis et al., 2018). In addition to the intentionally added plastic chemicals, plastics also include non-intentionally added substances (NIAS), that is, impurities of substances or additives, breakdown products, or manufacturing reaction by-products, all with unknown effects (Muncke et al., 2020). Both intentionally added chemicals and NIAS

constitute plastic food contact chemicals (FCCs), which refers to all the chemicals used in FCMs (Figure 1).

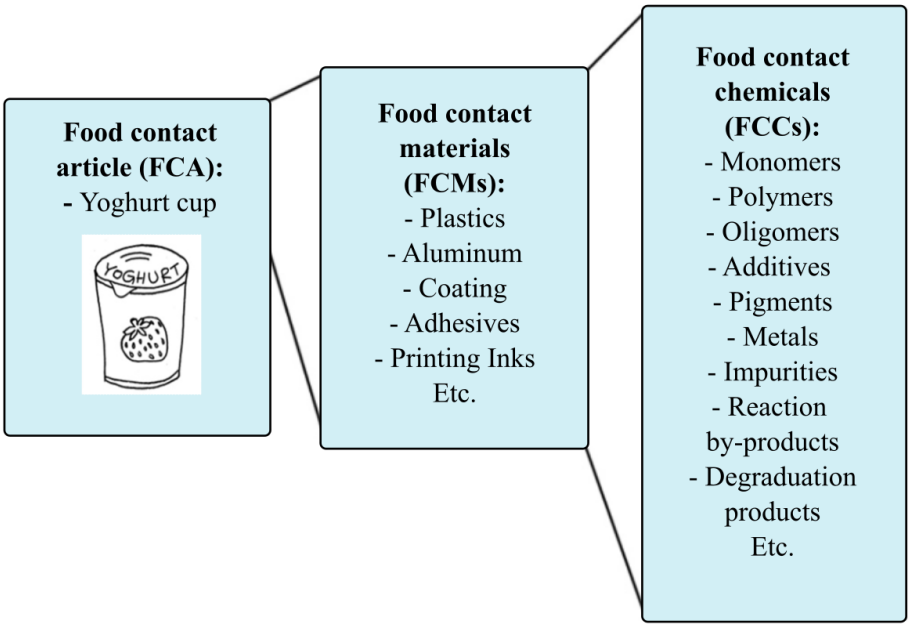

Figure 1: Schematic explanation of food contact article (FCAs), food contact materials (FCMs), and food contact chemicals (FCCs) (modified from Muncke et al., 2017).

Although these chemicals make FCMs, which hold great societal interest, FCCs can migrate from plastic packaging products into food (Muncke et al., 2017). For that reason, most humans are exposed to the FCCs via food intake. This is concerning because FCCs mimic our bodies natural chemicals and can thereby cause unwanted or harmful effects. For example, phthalates, plastic chemicals mainly used as plasticizers, and bisphenol A (BPA), a plastic chemical widely applied in consumer products such as reusable bottles or food containers, both have endocrine disrupting properties (Baralic et al., 2020). These chemicals can therefore interfere with the signaling pathways of hormones, either via metabolism, biosynthesis, or action, that can lead to adverse health effects, such as deviation from normal reproduction (Diamanti-Kandarakis et al., 2009). It has further been shown that other plastic packaging-associated chemicals, in addition to phthalates and BPA, have similar signaling disruptive properties (Wiesinger et al., 2021). This is because of the similar chemical structures often shared by plastic chemicals, specifically in instances where a harmful substance is substituted with a similar chemical to produce the same overall effect in the FCM (Moon, 2019). Substances that interact with signaling pathways are of concern as signal transduction from endogenous substances are crucial for proper cellular response.

In addition to harmful effects of plastic chemicals on signaling pathways, there are challenges regarding the risk assessment of plastic products (Muncke et al., 2017). Not only are very few plastic associated chemicals widely studied; systematical investigations of plastic products reveal that numerous chemicals are linked to concern regarding human health, and that many of these are barely or truly not studied (Groh et al., 2019, Wiesinger et al., 2021). In the European Union (EU), there are no clear regulations regarding NIAS. Risk assessments focus on the starting substances and additives, and thus, FCMs include numerous chemicals of unknown risk (Muncke et al., 2017). In addition to both the intentionally and unintentionally added chemicals in FCMs, the mixture effect caused by the presence of many chemicals is concerning as there are no regulatory requirements to quantify the effect of the mixtures (Muncke et al., 2020). Plastic chemical mixtures can induce toxicity despite none of the individual substances being toxic (Kortenkamp et al., 2007), and moreover, mixtures can cause toxicity greater than the additive effect of individual substances (Kortenkamp and Faust, 2018). Thus, mixture toxicity must be addressed to obtain knowledge on health impacts of FCCs (Muncke et al., 2020). This can be done by using whole migrate toxicity testing allowing for analysis of all chemicals in FCAs (Muncke et al., 2017, Zimmermann et al., 2021). Further, toxicants and agonists can be identified by combining bioassays to disclose activation of receptors by plastic chemicals and chemical analysis on specific plastic samples (Zimmermann et al., 2019).

With its many beneficial properties, plastic is a suitable material for a wide range of products. However, production of this material is constantly increasing, and with that there is a need to identify and classify the toxicity caused by plastic chemicals (Muncke et al., 2020).

1.2 G protein-coupled receptors

G protein-coupled receptors (GPCRs) are cell surface receptors that convey exogenous messages to the cell. They are subdivided into both classes and families. The classes, namely class A–F, are divided by their sequence homology and functional similarity, while the families, namely rhodopsin, secretin, glutamate, adhesion, and Frizzled/Taste2, are differentiated based on phylogenetics (Bjarnadóttir et al., 2006, Zhao et al., 2016). GPCRs are activated by a wide range of molecules, such as hormones, pheromones, neurotransmitters, photons, and odors (Heitzler et al., 2009, Zhao et al., 2016). As these receptors play crucial roles in numerous

physiological processes, such as sight, smell, and hormone stimulation, it is no surprise that GPCRs are common therapeutic targets (Wang et al., 2018). Being the largest and most diverse group of membrane receptors with approximately 800 members (Hauser et al., 2017), GPCRs are central in numerous functions that are crucial for exogenous signaling and cell–cell communication (Hanlon and Andrew, 2015). The olfactory GPCRs, comprising about half of the GPCRome, does not yet represent therapeutic targets, leaving about 400 GPCRs of interest in a pharmaceutical perspective (Hauser et al., 2017). Although the structure of GPCRs varies according to the numerous receptor functions, they have shared characteristics including seven membrane-spanning α-helixes that are separated by three intracellular and three extracellular loops (Figure 2, Rosenbaum et al., 2009).

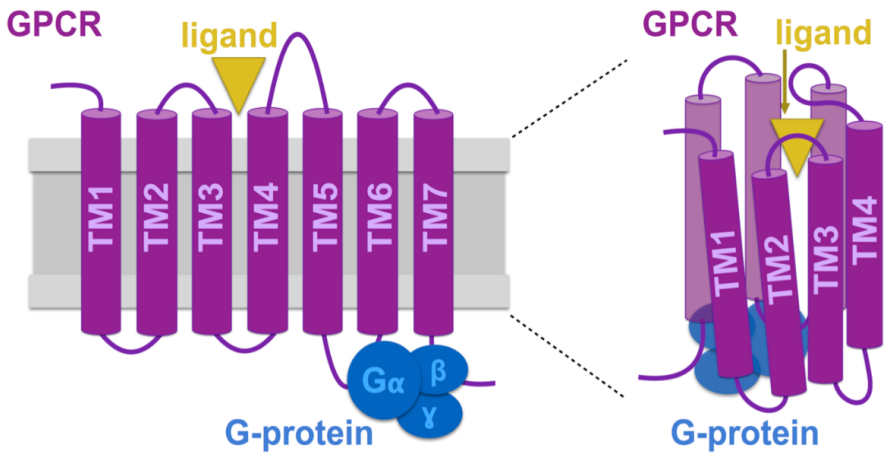

Figure 2: Illustration on the structure of G protein-coupled receptors, comprising seven transmembrane α-helixes and extracellular and intracellular loops. A more realistic organization of the receptor is shown on the right, while an unfolded overview is shown on the left (modified from Schneider et al., 2018).

The signaling through GPCRs is either G protein-dependent or G protein-independent (Heitzler et al., 2009). In short, the G protein-dependent pathway is initiated when the extracellular domain binds an agonist leading to the intracellular domain of the GPCR coupling to a G protein. When the G protein gets activated by the conformational changes of the agonist-binding GPCR, guanosine diphosphate (GDP) is replaced with guanosine triphosphate (GTP), leaving the G protein in an active state. The active subunits of the G protein (α, β, and γ) then conduct their duties leading to cellular responses such as interacting with enzymes to produce second messengers or regulating ion channels (Wang et al., 2018). The G protein-independent pathway is initiated when GPCR kinases (GRKs) phosphorylate the C-terminal end of the

GPCR in response to agonist binding. This phosphorylation recruits β-arrestin that has a key role in internalization and ubiquitination of the receptor (Figure 3, Tilley, 2012).

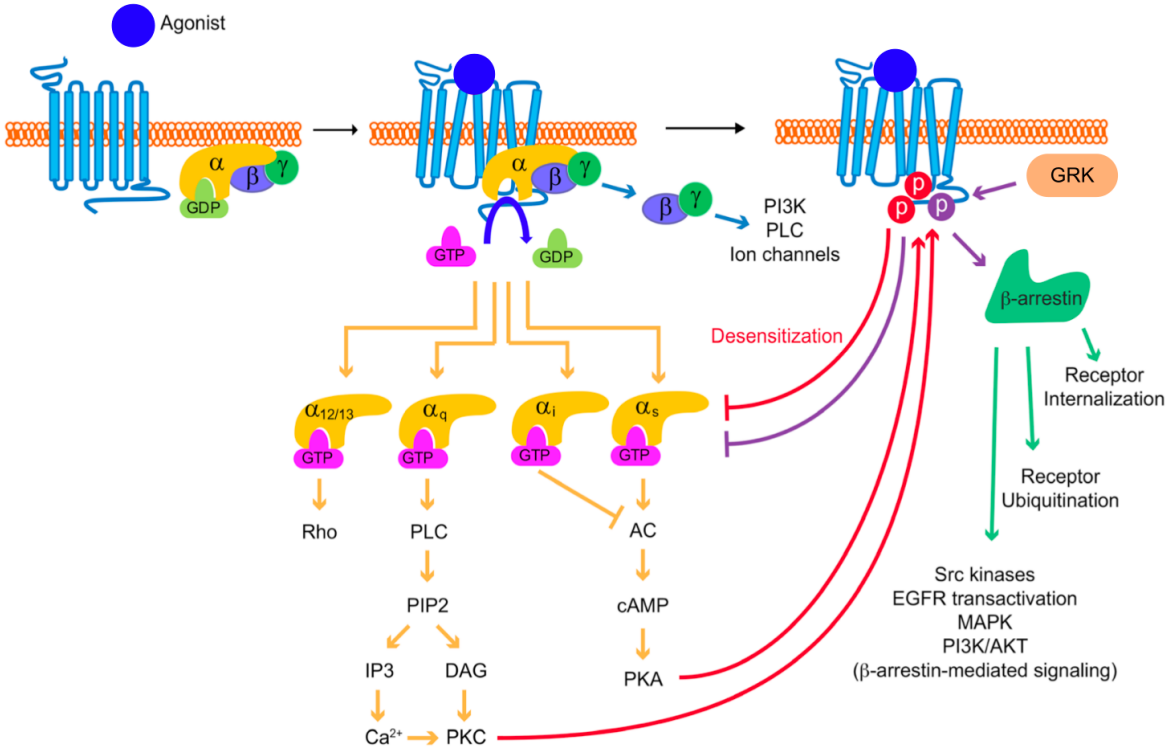

Figure 3: Illustration of G protein-coupled receptor (GPCR) signaling pathways (modified from Wang et al., 2018).

The two pathways of GPCR signaling are important pharmaceutical targets. Approximately 30% of approved drugs targets GPCRs as the primary target, and it is clear that an increased understanding of GPCRs have greatly affected modern medicine (Sriram and Insel, 2018). Previously, GPCR signaling was understood as a one-way route, meaning that GPCR activation of a G protein generated one specific cellular response (e.g., production of a second messenger) (Zhao et al., 2016). Later, the understanding of several G proteins and the distinguishment between G protein-dependent and -independent signaling have led to knowledge on GPCR signaling being more complex, such as the discovery of biased ligands, that is, ligands that favor either the dependent or independent GPCR pathway (Desimine et al., 2018). This discovery has been highly important in the pharmaceutical industry as one of the pathways may serve unfavorable side effects of a drug although the other pathway grants desired outcomes (Kolb et al., 2022). An example of an biased ligand is the μ-opioid receptor ligand oliceridine (TRV130) that does not interfere with the side effect inducing G protein-independent pathway

(Hauser et al., 2017). This shows that an extended understanding of druggable GPCRs is valuable in the reach to increase drug efficacy (Kolb et al., 2022).

Even though the importance of GPCR knowledge regarding drug discovery is clear, numerous receptors are still to be described. About 50% of the non-olfactory GPCRome is insufficiently studied. Precedent implies that the understudied and orphan GPCRs should have important signaling roles, and that many should be druggable (Rot and Kroeze, 2015). Since orphan GPCRs lack known ligands, and hence, the signaling pathway is unknown, approaching the G protein-independent pathways have been an important resource to increase knowledge on GPCR signaling and thus, understand cellular effects of these receptors (Rot and Kroeze, 2015, Sriram and Insel, 2018).

1.2.1 Environmental chemicals interfering with GPCRs

Proper GPCR activity is crucial for well-functioning cellular activities, and the consequences of disrupted signaling are as broad as the numerous functions of GPCRs. Examples are lack of sight, smell or taste, alternated mood and behavior, or insufficient hormonal stimulation (Rosenbaum et al., 2009). Despite the importance of GPCRs in physiological functions, they have not been widely studied in the field of toxicology as targets of environmental chemicals or endocrine disrupting chemicals. However, substances with wide applications can have GPCR-binding properties that have unfavorable health impact. For example, BPA, exerts estrogen-like activity through the G protein-coupled estrogen receptor (GPER, Pupo et al., 2012, Huang et al., 2021). Further, phthalates, can affect reproductive systems in young children. Exposure to phthalates via human breast milk have resulted in altered levels of important reproductive hormones such as the luteinizing hormone (LH), which signals through the GPCR luteinizing hormone receptor (Main et al., 2006, Jurewicz and Hanke, 2011). As plastics are more prevalent than ever, and emerging research has shown that plastic chemicals can interact with GPCRs resulting in potential unfavorable effects on human health (McPartland et al., 2022), an investigation on the effects of plastic exposure to GPCRs is of interest (Huang et al., 2021).

Building on our previous research which showed that plastic chemicals activate melatonin receptor 1A and 1B (MTNR1A and MTNR1B), serotonin receptor 1A and 2C (HTR1A and HTR2C), and adenosine receptor A_1 (ADORA1) (McPartland et al., 2022), this thesis investigated which polymers types and FCAs contain GPCR agonists. Although there is limited

research on the effect of environmental chemicals to these receptors, some of them have been targets of such chemicals. Carbaryl (1-naphthyl methylcarbamate) and carbofuran (2,3-dihydro-2,2-dimethyl-7-benzofuranyl methylcarbamate) are among the most toxic insecticides and show affinity to both MTNR1A and MTNR1B (Popovska-Gorevski et al., 2017, Glatfelter et al., 2021). Further, BPA exposure to rodents resulted in affected serotonin levels (Nakamura et al., 2010). Also, the plastic chemicals BPA and phthalates activate the ADORA1 receptor (Environmental Protection Agency, 2022). These findings indicate that environmental chemicals can disrupt GPCR signaling, and this supports that further investigation of GPCR disrupting chemicals in plastic FCAs is of interest.

1.2.2 Melatonin receptor 1A and 1B

The melatonin receptor 1A (MTNR1A) and 1B (MTNR1B) are the two melatonin-binding GPCRs in humans. Melatonin is often described as the "hormone of darkness" or the "biological marker of night" as it is synthesized and released at nighttime and in fact suppressed by light. The hormone is produced in the pineal gland and is rhythmically secreted, ensuring its involvement in circadian rhythms (Hardeland, 2012a). Even though melatonin is often connected to sleep, there is broad consensus that melatonin only has a small effect on sleep promotion, and that it is rather a biomarker of circadian rhythms and nighttime than a universal "sleep hormone" (Mirick and Davis, 2008, Foster, 2021). Melatonin is highly lipophilic, allowing it to reach most cellular compartments, and it has been linked to anti-inflammatory effects and antioxidative protection of cells (Foster, 2021). In addition, melatonin has an unambiguous role in the seasonal changes, such as coat thickness, reproductive status, and metabolism in some mammals (Hardeland et al., 2006).

Melatonin is detected by its target tissues through signaling via melatonin receptors. These receptors are widely expressed throughout the body, indicating broad sites of action. Even though both melatonin receptors are crucial in the synchrony of circadian clocks, the receptors seem to play different roles; MTNR1A inhibits neuronal activity while MTNR1B phase shift circadian firing rhythms in the suprachiasmatic nucleus, that is, a bilateral structure in the hypothalamus (Dubocovich, 2007). Melatonin deficiency or dysfunction of melatonin signaling can cause numerous sever consequences. Receptor knockout experiments on rodents have linked insufficient melatonin signaling to diseases such as cancer, diabetes types 2, mood disorders, and rheumatoid arthritis (Hardeland, 2012a).

1.2.3 Serotonin receptor 1A and 2C

Serotonin receptor 1A (HTR1A) and 2C (HTR2C) are neurotransmission mediating GPCRs that bind serotonin as their natural ligand. Serotonin is an important hormone and neurotransmitter in the central nervous system and participates in a variety of physiological processes such as intestinal movement, vomiting, and vasoconstriction (Sarkar et al., 2020). Further, the serotonergic signaling has a key role in several cognitive and behavioral functions including anxiety, depression, sleep, pain, mood, aggression, and learning. Serotonin has also been linked to wound healing as it acts as a growth factor in some cells (Żmudzka et al., 2018). Serotonin is commonly known as a wellness hormone. Along with dopamine its categorized as a "happy hormone", but whereas dopamine is released as an reward in response to pleasure, serotonin contributes to focused, emotionally stable, and calmer mental states, and would be released in response to contentment (Young, 2007).

Serotonin receptors modulate release of hormones such as cortisol, prolactin, and oxytocin, as well as neurotransmitters including dopamine, epinephrine, acetylcholine, and glutamate. Although both HTR1A and HTR2C share involvement in processes such as appetite, sexual behavior, and vasoconstriction, there are differences between the two. For instance, HTR1A decreases cellular cyclic adenosine monophosphate (cAMP) production, while HTR2C increases cellular level of calcium ions (Sharma, 2004, Felsing et al., 2018). As serotonin receptors affect a variety of biological and neurological processes, they are important drug targets, and particularly in treatment of psychiatric disorders, such as anxiety, migraine, hallucination, and depression (Żmudzka et al., 2018).

1.2.4 Adenosine A_1 receptor

The adenosine A_1 receptor (ADORA1) is a GPCR that is one of four adenosine receptors, and it is widely distributed in the body with adenosine as its endogenous ligand. Adenosine is an organic compound that holds a variety of functions, such as being one of the four nucleosides building RNA. Its derivates, adenosine mono-, di-, and triphosphate (AMP, ADP, and ATP), are vital energy carriers, and the second messenger cAMP, a derivate from ATP, is crucial in a variety of intracellular signaling pathways (Borea et al., 2018). In addition, adenosine protects tissue and organs in response to stress, and is for that reason described as a guarding angel. When a region undergoes high metabolism, and thus the oxygen demand is increased, adenosine interacts with the adenosine receptors to reduce oxygen demands in neurons and cardiomyocytes and increase vasodilation and oxygen delivery. This results in antithrombotic

properties and reduction of blood pressure and heart rate, giving adenosine therapeutic effects throughout most organ systems (Layland et al., 2014, Borea et al., 2018).

Adenosine receptors are common major targets of caffein and theophylline, that is, natural chemicals that ensures the stimulatory effect of coffee, chocolate, and tea. Later, their importance in tackling a variety of diseases has become understood (Jacobson and Gao, 2006). ADORA1 is an attractive therapeutic target for numerous diseases and conditions, such as heart failure, angina, arrythmias, stroke, depression, and diabetes. The receptor generally has inhibitory functions. In heart tissue, stimulation of the ADORA1 receptor has a depressant effect by reducing electrical impulses and inhibit pacemaker cell function. As a result, stimulation of ADORA1 by adenosine decreases heart rate, indicating that this is a suitable target for treating conditions involving fast heart rates (Layland et al., 2014). ADORA1 also has an important role in regulation of neurotransmitters in the brain, and it has been shown that this receptor is involved in physiological processes such as stroke, seizure, and sleep (Borea et al., 2018).

1.3 Rationale of the study

Plastic is a versatile material consisting of numerous plastic chemicals, both intentionally and unintentionally added (Muncke et al., 2017). As many of the substances in plastics are unknown, there is no way to know the health impacts of exposure (Muncke et al., 2020). Our group have previously shown that chemicals in plastic FCAs activate MTNR1A, MTNR1B, and ADORA1 (McPartland et al., 2022). However, these receptors were activated by substances in mixtures of chemicals extracted from multiple FCAs, and thus, the exact polymer type and plastic product responsible for the receptor activation remain unknown. Therefore, the aim of this study was to investigate which plastic FCAs contained the GPCR agonists. Based on previous work in our group, we hypothesized that PUR and PVC contain chemicals that would cause receptor activation on GPCRs, and in particular on MTNR1A and ADORA1 (McPartland et al., 2022).

To test these hypotheses, we aimed to; (1) validate the activity of samples from previous hits in our group, (2) identify which individual FCAs contained GPCR agonists, and (3) narrow down the list of potential agonists based on non-target chemical analysis.

2. Materials and methods

The experiments for this thesis were conducted in laboratories at the Norwegian University of Science and Technology (NTNU) Trondheim, Department of Biology. All materials and reagents are listed in Appendix A (Table A.1).

To investigate the agonism by plastic chemicals on GPCRs, plastic samples were extracted and analyzed using non-target chemical analysis to characterize the chemicals in each plastic sample. The plastic samples and GPCRs in this thesis were selected based on results from McPartland et al. (2022) describing the agonism that chemicals from two polymer mixes, namely "diverse polymer mix" and "PVC mix", induce at MTNR1A, MTNR1B, HTR1A, HTR2C, and ADORA1. The diverse polymer mix included three PE, two PP, two PS, and one PUR sample. The PVC mix included three PVC samples. Cytotoxicity tests for all samples were performed. To identify the individual FCAs which contained the active chemicals, we exposed the five mentioned GPCRs to plastic extracts in the PRESTO-Tango assay. The combination of non-target chemical analysis and cellular bioassays provided a holistic picture of the plastic chemical effects on the GPCRs investigated in this thesis.

2.1 Plastic extraction

2.1.1 Plastic samples

The eleven plastic samples for this thesis comprised the overall mixtures that activated the five previously mentioned receptors in the PRESTO-Tango assay (McPartland et al., 2022). The samples included five prevailing polymer types in today's market from countries with the highest waste per capita, and one additional sample from Norway (Table 1): PE, PP, PS, PUR, and PVC (PlasticsEurope, 2021).

2.1.2 Extraction

The extraction of the plastic samples was conducted by Sarah Stevens, Molly McPartland, and Hanna Sofie Skåland according to a previously established method (Zimmermann et al., 2019). Briefly, plastic samples were cut into pieces of 0.5–0.8 cm x 2 cm and placed in methanol-containing glass vials in a ratio of 20 mL methanol to 3 g plastic. The vials and a procedural blank (PB) consisting of only methanol (solvent) were extracted in an ultrasonic bath for 1 h at room temperature. The extracts (60 mL) were evaporated under a gentle stream of nitrogen. When the volume of the extracts reached 1 mL, they were transferred to clean 1.1 mL glass

vials for further evaporation of the solvent. Dimethyl sulfoxide (DMSO) was added in a volume of 600 µL, and the rest of the methanol was evaporated. The plastic extracts were stored at -20°C prior to cytotoxicity testing and PRESTO-Tango assays (Skåland, 2022).

2.1.3 Mixture of extracts

Two mixtures of plastic extracts were used in this thesis based on their observed activation at the MTNR1A and ADORA1 receptors (McPartland et al., 2022). The mixes were originally made enabling testing of a larger number of plastic samples than would have been possible with individual testing of each extract. As both mixes were active on ADORA1 and MTNR1A, the 11 extracts constituting the two mixes were selected for further evaluation using the PRESTO-Tango assay. To maintain the same total plastic concentration in the polymer mixes and individual plastic samples, the concentration of each individual sample was consequently eight times higher in the diverse polymer mix and three times higher in the PVC mix as compared to the individual samples. Previously, cytotoxicity testing had only been conducted for the polymer mixes, and thus, cytotoxicity tests were conducted for the plastic extracts in addition to both mixtures in this thesis (section 2.2).

Table 1: Information on plastic products investigated in this thesis. The number of chemical features in each plastic extract is derived from non-target chemical analysis.

Polymer mix	ID	Polymer type	Origin	Product	Number of features	Total number of features
Diverse polymer mix	PE1	Polyethylene	United States	Cling film	2790	25768
	PE2	Polyethylene	South Korea	Freezer bag	2607	
	PE3	Polyethylene	Germany	Freezer bag	3340	
	PP1	Polypropylene	South Korea	Coffee cup	2984	
	PP2	Polypropylene	United States	Yoghurt lid	3347	
	PS1	Polystyrene	United States	Styrofoam cup	3845	
	PS2	Polystyrene	Norway	Plate	2848	
	PUR	Polyurethane	Germany	Drinking bladder	4007	
PVC mix	PVC1	Polyvinyl chloride	United Kingdom	Cling film	5179	10785
	PVC2	Polyvinyl chloride	Germany	Drinking tube	3274	
	PVC3	Polyvinyl chloride	Germany	Drinking bladder tube	2332	

2.2 Cytotoxicity testing

Cytotoxicity testing of all polymer mixes and individual plastic extracts were conducted in four experiments to quantify the viability of HTLA cells exposed to seven concentrations of each plastic extracts. This was done to compare the cytotoxicity of polymer mixes and individual plastic samples, and to determine the concentration of plastic samples in the PRESTO-Tango assay. The plates for these experiments were seeded and exposed to plastic extracts as described in section 2.3.3. However, several notable differences are important. First, all cytotoxicity experiments were conducted on non-transfected cells and therefore, nuclei count data was used as a measure of cell viability and cytotoxicity quantification. After 23 h of exposure, the solution was replaced with 25 µL PBS: NucBlue (R37605, Invitrogen) staining solution (50 µL NucBlue per mL PBS). The plate was incubated at room temperature for 30 min before the NucBlue staining solution was replaced with 25 µL of PBS. The wells of the plate were imaged by a Cytation 5 Cell Imaging Multimode Multimode reader (BioTek) with a 4x Plan Fluorite objective (WD 17 NA 0.13) using a 365 LED with DAPI filter cube (Ex 377/50, Em 447/60). Note that column 12 and 13 of the plate is marked "SC/NC" because a solvent control not being included in the first two experiments, and rather two negative controls were present (Figure 4).

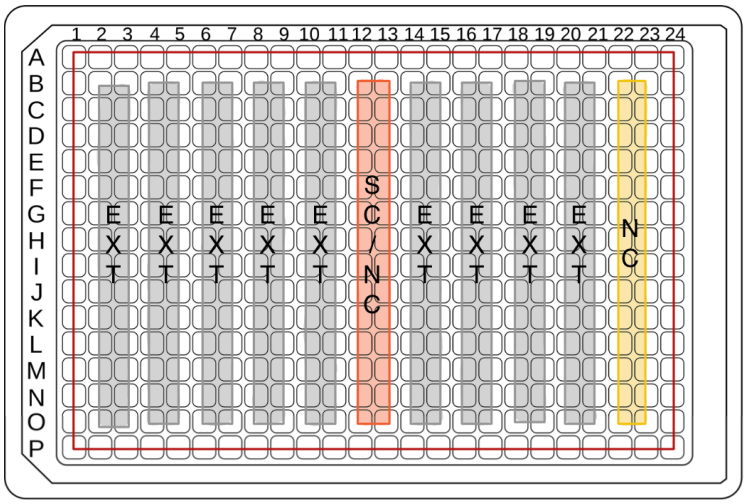

Figure 4: Plate layout for HTLA cells treated with to plastic extracts (EXT), negative control (NC), and solvent control (SC).

2.3 PRESTO-Tango Assay

The PRESTO-Tango assay was used to quantify the possible agonism of plastic extract chemicals on GPCRs. All GPCR plasmids were isolated from unique *Escherichia coli* (*E. coli*) glycerol stocks in preparation for the assay (Addgene, Kit #1000000068). HTLA cells, HEK293 cells expressing a tethered transcriptional activator (tTA) dependent luciferase reporter and a β-arrestin2-tobacco etch virus (TEV) protease fusion gene stably, were cultured to obtain optimal confluency prior to the assay (60-80%) and transfected with the desired GPCR construct. HTLA cells were kindly provided by Brian Roth.

The PRESTO-Tango method is a modification of the Tango-method, that is based on measurement of G protein-independent β-arrestin recruitment that occurs in connection to the desensitization of GPCRs (Figure 5). This method differs from previous GPCR screening methods by utilizing the G protein-independent pathways of the signaling, and not the coupling of GPCRs to G proteins (Dogra et al., 2016). The independence from G protein coupling is a great advantage in the investigation of the druggable GPCRome because GPCRs can be investigated simultaneously enabling application to all GPCRs, including orphan GPCRs with unknown coupling partners. The general principle of the PRESTO-Tango assay is much like the Tango method, however, it includes some changes such as the design of the plasmid constructs and the assay execution making it suitable for encompassing essentially the entire human druggable GPCRome (Kroeze et al., 2015).

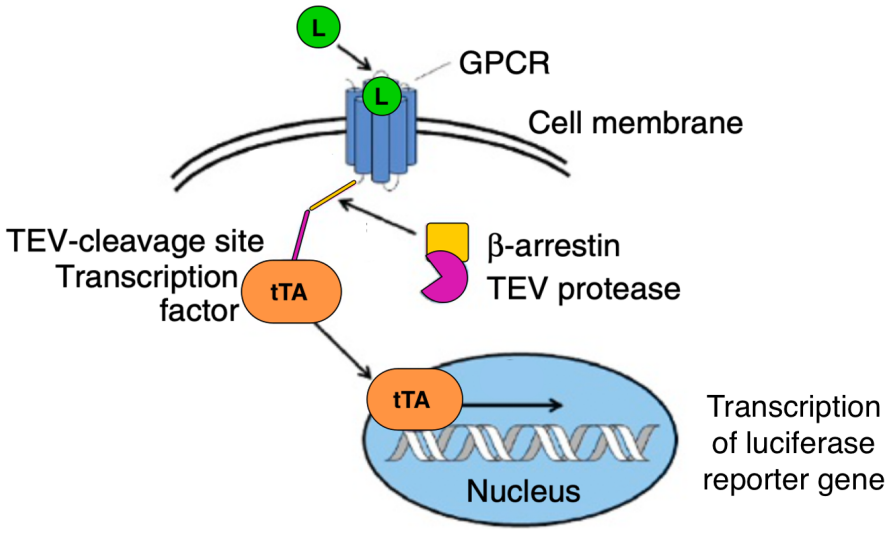

Figure 5: Schematic presentation of the PRESTO-Tango assay including a G protein-coupled receptor (GPCR), ligand (L), β-arrestin, tobacco etch virus (TEV) protease, and tethered transcriptional activator (tTA) (modified from Kroeze et al., 2015).

2.3.1 Plasmid production and isolation

The plasmid purification was performed to isolate DNA containing the desired plasmid for each receptor utilized in this thesis. Plasmid isolation from *E. coli* was performed with Wizard Plus Midipreps DNA Purification System (A7640, Promega) with some adjustments for available equipment. The kit included all reagents needed for the isolation: Cell Resuspension Solution, Cell Lysis Solution, Neutralization Solution, Wizard Midipreps DNA Purification Resin, Column Wash Solution, and Nuclease-Free Water.

All midipreps were carried out as described by the manufacturers protocol (Promega, 2010) with some notable exceptions. Briefly, *E. coli* producing the relevant plasmid (MTNR1A, MTNR1B, HTR1A, HTR2C, or ADORA1) were picked with a sterile pipette tip and placed in 70 mL liquid lysogeny broth (LB) medium (Appendix A, Table A.6) with 70 µL ampicillin in a baffled Erlenmeyer flask. The bacteria culture was placed in a shaking incubator for 18-20 h at 37°C and 200 rpm. Proper bacteria growth was characterized by a cloudy haze in the media as compared to a clear control.

After incubation, the bacteria culture was pelleted in a 50 mL centrifuge tube by centrifugation in a Heraeus Megafuge 1.0R centrifuge (D-37520, Kendro Laboratory Products) at 10,000 x *g*

at 4°C for 10 min. The supernatant was carefully discarded, and the pellet was resuspended in 3 mL of Cell Resuspension Solution. Cell Lysis Solution (3 mL) was mixed by inverting the tube four times. The tube was incubated at room temperature for 3 min before 3 mL of Neutralization Solution was mixed by inverting the tube four times. The tube was then incubated again at room temperature for 10 min, followed by a centrifugation at 10,000 x *g* at 4°C for 20 min. The DNA containing supernatant was carefully transferred to a new 50 mL centrifuge tube, and 10 mL of Wizard Midipreps DNA Purification Resin was added. The tube was swirled to mix the liquids. A Wizard Midicolumn was inserted to a vacuum manifold port, and the resin/DNA mixture was transferred to the midicolumn. A vacuum of 508 mbar was applied until the liquids were pulled through the filter of the column. The column was washed twice with 15 mL of Column Wash Solution. The resin was dried by continuing to draw the vacuum for 30 sec after the Column Wash Solution was pulled through the filter. The reservoir was then separated from the midicolumn and transferred to a 1.5 mL microcentrifuge tube. The midicolumn was centrifuged at 10,000 x *g* for 2 min in a VWR Micro Star 17 centrifuge (521-1646, VWR) before the column was transferred to a new microcentrifuge tube and 300 µL of Nuclease-Free Water (preheated to 70°C) was left on the midicolumn for 1 min. DNA was eluted by centrifuging the tube at 10,000 x *g* for 20 sec. The midicolumn was removed, and the microcentrifuge tube was centrifuged at 10,000 x *g* for 5 min. The DNA-containing supernatant was carefully transferred to a new microcentrifuge tube. Plasmid concentrations were analyzed on a NanoDrop 2000c Spectrophotometer (Thermo Scientific) and stored at -20°C.

2.3.2 Cell culturing

HTLA cells cultured at passage 4 were used in this study. Thawed cells (1 mL) were pipetted into a T75 tissue culture flask containing 19 mL of growth media (Appendix A, Table A.2). The next day the growth media was exchanged and spiked with selection markers (puromycin 2 µg/mL and hygromycin 100 µg/mL).

Cells were passaged when confluency reached 70%. This was done by aspirating growth media from the T75 tissue culture flask and carefully rinsing cells with 10 mL of prewarmed phosphate-buffered saline (PBS, Appendix A, Table A.4) twice. To detach the cells from the flask, 1 mL of trypsin solution was added, and the flask was incubated for 5 min before 9 mL prewarmed growth media was added to get the desired split ratio of 1:10. The side of the flask was rinsed multiple times with the growth media before potential cell clumps were separated

by pipetting the solution while pressing the tip of the pipette against the bottom of the flask. In a new, sterile T75 tissue culture flask, 1 mL of trypsinated cell solution was added to 11 mL selection media. The cells were incubated at 37 ºC with 5% CO_2 in humidified conditions. The day after passaging the cells, the growth media was exchanged with 12 mL of prewarmed, selection media. The cells were observed with a Nikon Eclipse TS100 microscope to ensure proper growth before and after every treatment of either passaging or media exchange. Cells were discarded when irregular growth patterns emerged (such as cell growth in layers or noticeably slow or fast cell growth), or after passage 25. Note that for some days, the split ratio was reduced to ensure proper cell confluency for experiments.

2.3.3 Bioluminescence assay

The PRESTO-Tango assay was carried out with HTLA cells transfected with each of the five receptors used in this thesis, and the cells were exposed to plastic extracts of five polymer types (Table 2). The four main steps of the PRESTO-Tango assay (seeding, transfection, treatment, and luminescence read) are further described in this section.

Table 2: Overview of reference compounds and plastic extract treatment for the five receptors investigated in this thesis. Note that the receptor-sample concentrations were selected based on previous hits in the PRESTO-Tango assay.

Receptor	Reference compound	Purity, CAS number, and supplier of PC	Solvent	Plastic extract treatment
MTNR1A	Melatonin (1 x 10^{-5} – 10 µM)	>98%, 73-31-4, Sigma-Aldrich	DMSO	PVC1–3
MTNR1B	Melatonin (1 x 10^{-5} – 10 µM)	>98%, 73-31-4, Sigma-Aldrich	DMSO	PVC1–3
HTR1A	Lysergic acid diethylamide (LSD, 1 x 10^{-5} – 10 µM)	>99%, 50-37-3, Chiron	DMSO or methanol	PE1–3, PP1–2, PS1–2, PUR
HTR2C	Lysergic acid diethylamide (LSD, 1 x 10^{-5} – 10 µM)	>99%, 50-37-3, Chiron	Methanol	PE1–3, PP1–2, PS1–2, PUR
ADORA1	5′-N-ethylcarboxamide adenosine (NECA, 1 x 10^{-5} – 10, 3 x 10^{-5} – 30, or 5 x 10^{-5} – 50 µM)	>99%, 35920-39-9, abcam	DMSO	PVC1–3
ADORA1	5′-N-ethylcarboxamide adenosine (NECA, 1 x 10^{-5} – 10, 3 x 10^{-5} – 30, or 5 x 10^{-5} – 50 µM)	>99%, 35920-39-9, abcam	DMSO	PE1–3, PP1–2, PS1–2, PUR

2.3.3.1 Seeding the cells (day 1)

A 384-well plate containing 20 µL of 0.1 mg/mL poly-L-lysine (PLL, Sigma Aldrich, P2636) in each well was left in room temperature for 1.5 h before the PLL was removed by flicking the liquid out of the plate and tapping it on tissue paper. HTLA cells with a confluency of 70% were trypsinated, and the cell number was determined using a cell counter (BIO-RAD TC20 Automated Cell Counter, with gates at 10–18 µm). With a desired number of 7000 cells per well and 1.54 x 10^5 cells/mL, the number of cells needed was calculated as following:

$$\frac{1.54\ x\ 10^5 cells/mL}{counted\ cells/mL}\ x\ 22\ ml = volume\ (mL)\ of\ cells\ needed$$

The calculated volume of cell suspension was mixed with prewarmed growth media in a volume to make 22 mL, and 45 µL was seeded in each well of the 384-well plate. The plate was incubated at 37 ºC with 5% CO_2 in humidified conditions for 24 h.

2.3.3.2 Transfection of the cells (day 2)

The day after the seeding, HTLA cells were transfected with the respective plasmid using the Lipofectamine 3000 method according to the manufacturer's instruction (L3000008, ThermoFisher). In brief, the plasmid DNA was suspended in 0.1x Tris-EDTA (TE) buffer (Appendix A, Table A.5) to obtain a concentration of 50 ng/µL. Growth media was replaced with 30 µL prewarmed growth media. DNA-lipid complex for each plasmid DNA type was prepared according to the number of wells being transfected (Appendix B, table B.1). DNA-lipid complex (10 µL) was added to each well of a 384-well plate, and the plate was incubated at 37 ºC with 5% CO_2 in humidified conditions for 24 h.

2.3.3.3 Cell treatment (day 3)

The transfection media was replaced with 30 µL starving media (Appendix A, Table A.3). The plate was incubated for 30 min while plastic extracts and control compounds were prepared (Appendix B, Table B.2). The reference compounds had original concentrations of 10 or 20 mM and were diluted in starving media to obtain the highest concentrations of 10, 30 or 50 µM. These concentrations were further diluted 1:10 in a dilution series with six steps. All plastic extracts had original concentrations of 30 mg plastic/µL. These were diluted 1:250 in starving media, and further diluted 1:2 in six steps with the highest plastic concentration being 1.8 mg

plastic/well. The exception was PUR which, based on cytotoxicity, was diluted from the original concentration of 30 mg plastic/µL to obtain the highest PUR concentration of 3.75 x 10^{-2} mg plastic/well and further diluted 1:2 in six steps. Treatment solution was well mixed and 30 µL was added to each well, and the plate was incubated at 37 ºC with 5% CO_2 in humidified conditions for 23 h.

2.3.3.4 Luminescence reading (day 4)

After 23 h, the treatment solution was removed, the cells were washed twice with 25 µL PBS, and 20 µL Cell lysis mix was added to lyse the cells (Appendix A, Table A.7). A white sticker was placed underneath the plate on the transparent bottom before being read in a Cytation 5 Cell Imaging Multimode Multimode reader (BioTek) with a 4x Plan Fluorite objective (WD 17 NA 0.13). The plate was shaken for 3 min to ensure lysis of the cells and luminescence was measured for one second for each well after injection of 30 µL luminescence mix (Appendix A, Table A.8) before the reaction was quenched with 30 µL NaOH 8 g/L.

2.3.4 Plate layout for the PRESTO-Tango assay

To optimize the assay procedure according to the plastic chemicals, receptors, and equipment available, some factors were changed throughout the duration of this thesis. To avoid using multiple different plate layouts, the factors that were changed were implemented at the same time at experiment 9. Accordingly, two different layouts were used for experiments 1–8 and 9–21 (Figure 6).

In the first eight experiments, we observed a "bleeding" effect in the luminescence measurements in the same pattern as the plate was read, resulting in apparent activation where there was none. For this reason, each treatment (either positive control, solvent control, or plastic extract) was plated with two columns in between each other to avoid the bleeding effect as much as possible (Figure 6A). An edge effect was also observed for the first eight experiments, which refers to significant differences in the outside wells (predominantly lower luminescence) than in the inner wells most often caused by evaporation or lower cell numbers (Mansoury et al., 2021). Lastly, the first eight experiments only included a negative control and not a solvent control. However, a background was included on each plate which consisted of both a negative and solvent control for the un-transfected HTLA cells.

To correct these effects, the following changes were made from experiments 9 to 21 (Figure 6B):

1. The direction of the plate reader was changed from horizontal to vertical reading to minimize bleeding between samples.
2. A pause of 20 seconds was added between samples to provide more time for the quenching solution to minimize luminescence in previously read wells.
3. The outer wells were no longer used, and solvent controls were included for transfected cells as well.

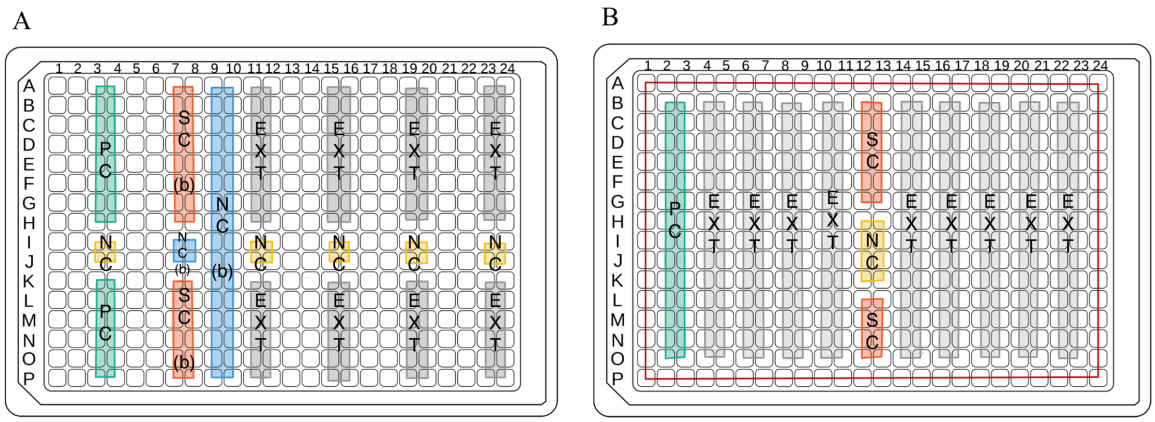

Figure 6: Plate layouts for HTLA cells exposed to plastic extracts (EXT), negative control (NC), negative control on background (NCb), positive control (PC), solvent control (SC), and solvent control on background (SCb) in the PRESTO-Tango assays conducted in this thesis. (A) Plate layout for experiments 1–8. **(B)** Plate layout for experiments 9–21.

2.4 Non-target chemical analysis of extracts

To obtain a more in-depth understanding of the chemical composition of the different polymer types analyzed in this thesis, ultra-high performance liquid chromatography (Acquity UPLC I-Class, Waters) coupled to a quadrupole time-of-flight mass spectrometer (Synapt G2-S HDMS, Waters) was performed by Hanna Sofie Skåland (Skåland, 2022). The resulting dataset included quantity of chemical features detected in each sample (Table 1) and was further analyzed in this thesis to identify potential GPCR agonists.

2.5 Data analysis

2.5.1 Software

To perform the statistical analysis and create figures for this thesis, the free statistical computing and graphics software, RStudio (RStudio, 2022.07.1 Build 492) was used. Specific functions used for each calculation are mentioned throughout this section. All R packages used are listed in Appendix C. Microsoft Excel (version 16.65, 22091101) was used to compile and filter raw data, and Inkscape (version 1.2, dc2aeda, 2022-05-15) was used for aesthetic adjustments of the figures (e.g., font sizes).

2.5.2 Cytotoxicity data analysis

The number of cells were counted from the images taken by the Cytation 5 Cell Imaging Multimode Multimode reader using a Cell profiler pipeline (Stirling et al., 2021). The pipeline counted the cells based on nuclei stained with NucBlue. The cell count of the different treatments and concentrations were normalized to the negative control by dividing the cell count on the mean of the negative control. As a solvent control was not included in the first two experiments, a Wilcoxon signed-rank test (described in section 2.5.4.1) could not be performed to exclude any cytotoxicity effect of the solvent for these plates. In the last two experiments, however, a solvent control was included, and the Wilcoxon signed-rank test was conducted confirming that there was no overall cytotoxic effect of the solvent. The figures presenting the cytotoxicity results were made using the *ggplot()* function by plotting the normalized cell count against the seven concentrations of the different plastic samples. The plastic extracts were fitted using a three-parameter log-logistic concentration-response model from the *drm()* function, where the lower limit of the concentration-response curve was constrained to zero. Plastic extract concentrations resulting in cell viability below 80% of the mean negative control were considered cytotoxic.

2.5.3 PRESTO-Tango assay analysis

All luminescence measurements from the PRESTO-Tango assay were normalized to the positive control for each receptor. The normalization was done using the following equation, with constitutive activity equaling the mean of solvent control and negative control, and PC indicating the positive control:

$$Normalized\ data = \frac{Luminescence, plastic\ extract - constitutive\ \ activity}{Luminescence, upper\ limit\ PC - constitutive\ activity} * 100$$

The figures illustrating the results from the assays were made using the *ggplot()* function by plotting normalized luminescence values to the seven concentrations of plastic samples. The plastic extracts were fit using a four-parameter log-logistic concentration-response model from the *drm()* function.

2.5.4 Quality assurance analysis

Quality assurance of the data included a positive control for each receptor that was evaluated based on a sigmoid concentration-response relationship, a Z-factor, and a Wilcoxon signed-rank test. For all active extracts, three biological replicates (i.e., independent experiments) were conducted to ensure repeatability of results. For inactive extracts only two biological replicates were conducted to confirm the null result. All biological replicates include four technical replicates.

2.5.4.1 Solvent effect

The Wilcoxon signed-rank test was used to exclude the solvent used for the plastic extractions as a source of receptor activation in the PRESTO-Tango assays (Conover, 1999). A negative control and a solvent control were included in each experiment, and the luminescence in the two controls were compared statistically. The Wilcoxon signed-rank test was performed on cells exposed to the controls on un-transfected cells in experiments 1–8, and on transfected cells in experiment 9–21 (Figure 6). A p value > 0.05 indicated no activation by the solvent control and was therefore accepted as a measure of receptor activation by the plastic extract chemicals. The calculations were performed in R Studio using the *Wilcox.test()* function, and the function calculates the p value based on vectors of the two treatments.

2.5.4.2 Assay quality

Z-factor is a measure of the statistical effect size of an assay. An assay with a Z-factor between 0.5 and 1 is described as excellent, and an assay scoring between 0 and 0.5 as marginal but acceptable. Any assay with a Z-factor below 0 is described as unacceptable (Zhang et al., 1999). While Z-factor rankings of assays are predominantly meant for pilot screens to predict the suitability and quality of a high-throughput screening assay, it was used in this thesis to assess the validity of the experiment. Therefore, a Z-factor below 0 did not directly cause the experiment to be considered unacceptable. However, Z-factors below 0 were considered to

indicate poorer quality of the experiment in question, and experiments where half maximal effective concentration (EC_{50}) values could not be calculated (confirmed by extremely low Z-factors and visual inspection) were not accepted to measure plastic extract activation on the receptors. The Z-factor score of the experiments was calculated in R studio based on the following equation with the parameters mean (μ) and standard deviation (σ) of the negative control (n) and of the highest concentration of the reference compound (p).

$$Z - factor = 1 - \frac{3(\sigma_p + \sigma_n)}{|\mu_p - \mu_n|}$$

2.5.4.3 Positive control concentration-response curve

The positive control concentration-response curves were created using the *ggplot()* function. Fold activation of the positive control was calculated for each concentration by dividing the measured luminescence of the reference compound on the constitutive activity (the luminescence of the negative control and the solvent control). Fold activation induced by the reference compound was fitted using a four-parameter log-logistic concentration-response model from the *drm()* function. The concentration-response curves were visually inspected, and any experiments with a positive control concentration-response curve that did not meet the requirement of a sigmoid shape was not considered for further analysis. EC_{50} values were retained from the positive control model in R studio.

2.5.4.4 PRESTO-Tango assay evaluation

The concentration-response curves of plastic extract treatment were categorized as either True or False based on whether the plastic extract was active or not at the highest concentration. For a curve to be categorized as true, activation above the limit of detected (LOD) was expected. The LOD was calculated by adding three times the standard deviation of the solvent and negative control to the mean of these controls. The active samples were concluded to contain plastic extract chemical agonists for the receptor being tested.

2.5.5 Non-target chemical analysis

The chemical data included the molecular weight mass per charge (*m/z*) and the abundance for each chemical feature of the plastic samples (n = 11). Only features that were absent in the procedural blanks or had an at least 10-fold higher raw abundances were included in the

analyses. Additional filtering to narrow down possible agonists was conducted in Excel using the filtering function and was done to find features with an abundance ≥ five times of that in the inactive samples. Features with high abundancies in the active plastic samples were considered likely to cause the agonism. The data was converted to a matrix and heatmaps were created using the *pheatmap()* function in R studio with clustered columns and rows.

3. Results

3.1 Cytotoxicity testing

Cytotoxicity tests were performed for each plastic sample and polymer mix to investigate the cell viability of HTLA cells exposed to concentrations of the plastic extracts. The findings were used to explore the cytotoxicity of polymer mixtures compared to individual plastic samples, and further, they were used to ensure that plastic extract concentrations in the PRESTO-Tango assay were not cytotoxic. Wilcoxon signed-rank tests comparing the solvent control and negative control in the last two experiments resulted in p values of 6.64×10^{-8} for experiment 3 and 0.021 for experiment 4 (Table 3). These were both below the threshold of 0.05, indicating significant differences in cell viability between the controls. Note that the overall cell viability for the cells exposed to the solvent control was higher than for negative control cells (Figure 7). Only the highest concentration of the solvent induced a decrease in cell count. This indicates that for all concentrations except the highest, the solvent did not reduce cell count despite the low p value from the Wilcoxon signed-rank test. This can rather be observed as a slight proliferative effect on the cells.

Table 3: Overview of the set up for four cytotoxicity experiments conducted for this thesis.

Exp. number	Treatment	Wilcoxon signed-rank test, p value
1	Diverse polymer mix, PE1–3, PP1–2, PS1–2, PUR + negative control	-
2	PVC mix, PVC1–3 + negative control	-
3	Diverse polymer mix, PE1–3, PP1–2, PS1–2, PUR + negative control + solvent control	6.64×10^{-8}
4	PVC mix, PVC1–3 + negative control + solvent control	0.021

3.1.1 Individual plastic extracts

PE 1 and PE 3 were both cytotoxic. The cell viability for PE 3 was lower than for PE 1. For PE 1, only the highest concentration of plastic treatment (9 mg plastic/well) resulted in cell viability below 80% of the negative control, while both the highest and the second highest PE 3 concentrations (≥ 4.5 mg plastic/well) resulted in cytotoxicity. PE 2 did not induce cytotoxicity (Table 4, Figure 7A). The highest concentration (9 mg plastic/well) of PP 1 was cytotoxic, while both the highest and the second highest concentrations (≥ 4.5 mg plastic/well) of PP 2 induced cytotoxicity. PP 2 treatment resulted in lower cell viability than PP 1 (Table 4, Figure 8B). The highest concentration (9 mg plastic/well) of PS 2 resulted in cell viability below the threshold for cytotoxicity (Table 4, Figure 7C). PS 1 did not induce cytotoxicity. PUR was the most cytotoxic of the plastic samples. Note that the seven concentrations of PUR are 60 times lower than the other polymer types to account for very high cytotoxicity as compared to the

other plastic samples. The two highest concentrations of PUR (0.075 and 0.15 mg plastic/well) that were tested induced cytotoxicity (Table 4, Figure 7D). The highest concentration (9 mg plastic/well) of all three PVC samples were cytotoxic (Figure 7E). In addition, treatment to the second highest concentration (4.5 µM) of PVC 2 also induced cytotoxicity. PVC 2 was the most cytotoxic PVC sample followed by PVC 3 and then PVC 1 (Table 4, Figure 7E).

3.1.2 Polymer mixes

The diverse polymer mix was cytotoxic at the two highest concentrations (9 mg plastic/well and 4.5 mg plastic/well, Figure 7, A–D). The PVC mix was cytotoxic for the three highest concentrations (9 mg plastic/well, 4.5 mg plastic/well, and 2.25 mg plastic/well, Figure 7E). Both polymer mixes induced more cytotoxicity than any of the individual plastic sample, except for PUR.

Table 4: Overview of cytotoxicity results of HTLA cells exposed to plastic samples (n = 13) of five polymer types. The plastic samples are categorized as True/False based on cytotoxicity induction of the highest plastic extract concentration (9 mg plastic/well). EC_{20} values are listed for cytotoxic samples.

Extract/mix	Cytotoxic at highest concentration	Highest non-cytotoxic concentration (mg plastic/well)	EC_{20} (mg plastic/well)
Diverse polymer mix	True	2.250	2.123
PE1	True	4.500	6.213
PE2	False	9.000	7.444
PE3	True	2.250	3.812
PP1	True	4.500	4.635
PP2	True	2.250	3.645
PS1	False	9.000	7.208
PS2	True	4.500	6.192
PUR	True	0.038	0.052
PVC mix	True	1.125	2.585
PVC1	True	4.500	8.502
PVC2	True	2.250	3.037
PVC3	True	4.500	7.934

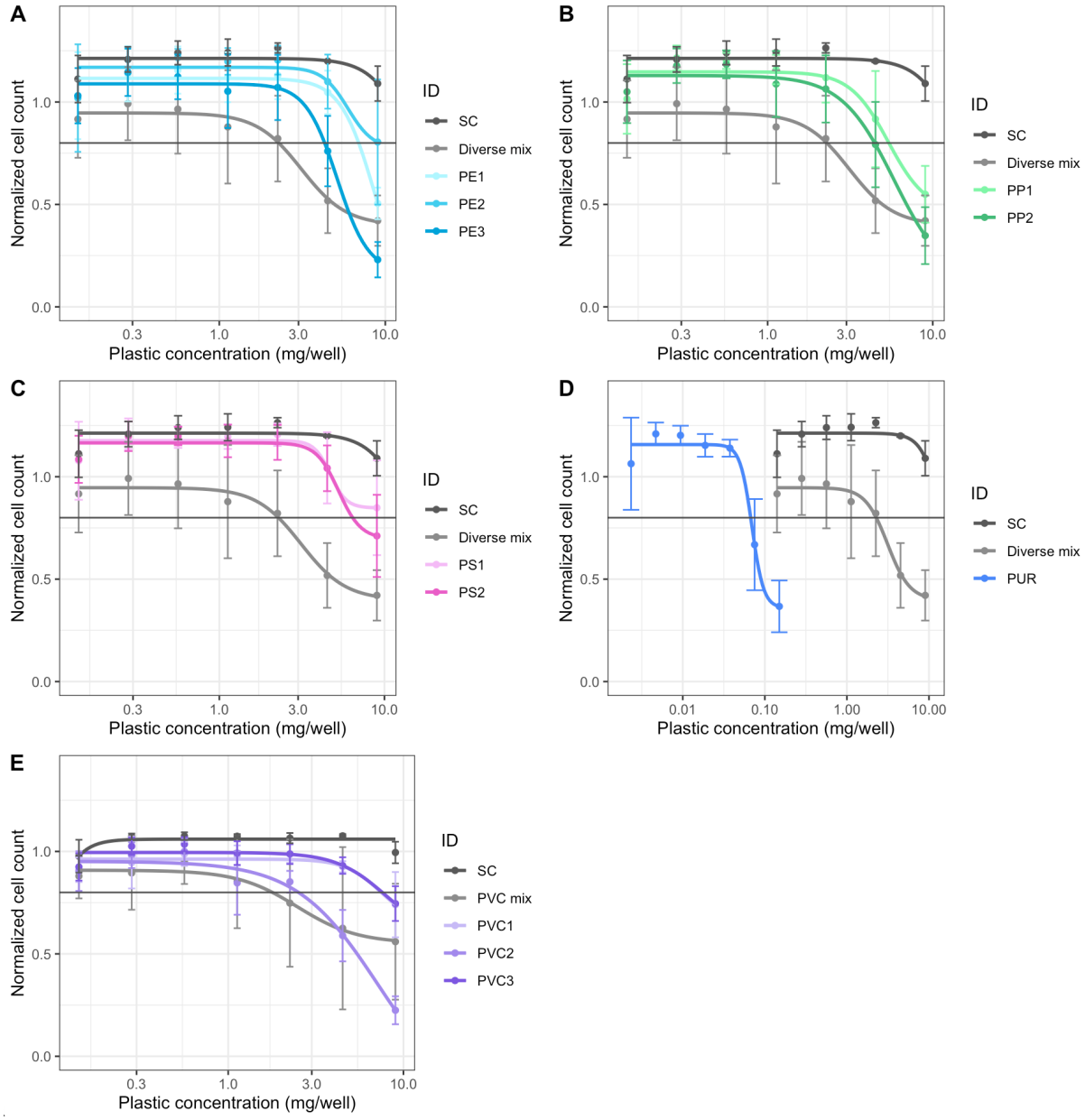

Figure 7: Cytotoxicity in HTLA cells exposed to plastic extracts (n = 6–8). All subfigures include concentration-response curves for a solvent control (SC, dark grey) and for a polymer mix the given extract was included in (lighter grey). The straight, horizontal line represents 80% of the mean cell viability for the negative control and represents the cytotoxicity threshold. Note that the treatment concentration of PUR is 60 times lower than the other plastic extracts. **(A)** Polyethylene (PE) treatment. **(B)** Polypropylene (PP) treatment. **(C)** Polystyrene (PS) treatment. **(D)** Polyurethane (PUR) treatment. **(E)** Polyvinyl chloride (PVC) treatment.

3.2 PRESTO-Tango reporter gene assay

The PRESTO-Tango assay was conducted to investigate agonism of 11 plastic samples on 4 GPCRs. Each assay included a positive control that fulfilled three quality criteria and was therefore used to guarantee quality of the data. The three criteria were the Wilcoxon signed-rank test, calculation of Z-factor, and checking for sigmoid concentration-response curve.

3.2.1 Solvent effect

The Wilcoxon signed-rank test was performed to exclude possible effects the solvent may have on the bioassay. The experiments with a resulting p value > 0.05 from the Wilcoxon signed-rank test indicate no effect of the solvent on the bioassay and were therefore included in this thesis. Of the 21 experiments conducted, 14 (70 %) were included. However, p value < 0.05 indicates a possible effect of the solvent and, therefore, the results of experiments 4, 11, and 13 ($p = 0.012$, 6.44×10^{-7}, and 7.72×10^{-6}, respectively) were not considered for assessing the receptor activation by plastic extracts (Table 5).

Table 5: Overview of the 21 PRESTO-Tango assays conducted for this thesis, including quality assurance parameters. Note that some experiment numbers are repeated (experiment 3 and 12) as the plate for the given experiment fitted more than one receptor. Abbreviations: MT = Melatonin, ATP = Adenosine Triphosphate, NECA = 5′-N-ethylcarboxamide adenosine, LSD = Lysergic acid diethylamide. Two of the receptors in experiment 12 have no plastic treatment ID because the experiment was for establishing the positive control only.

Exp. number	Receptor	Plastic treatment	Reference compound (highest concentration)	Effect of solvent vs negative control (p value)	Z-factor	Acceptable shape of concentration-response relationship	EC_{50}, positive control (µM)
1	MTNR1A	PVC1–3	MT (10 µM)	0.109	0.663	Pass	1.75×10^{-4}
2	MTNR1A	PVC1–3	MT (10 uM)	0.816	0.708	Pass	2.29×10^{-4}
3	MTNR1A	PVC1–3	MT (10 uM)	0.526	0.408	Pass	1.64×10^{-4}
3	MTNR1B	PVC1–3	MT (10 uM)	0.526	0.371	Pass	3.75×10^{-3}
4	MTNR1A	PVC1–3	MT (10 uM)	0.012	0.790	Pass	1.71×10^{-4}
5	MTNR1B	PVC1–3	MT (10 uM)	0.909	0.779	Pass	2.61×10^{-3}
6	ADORA 1	PE1–2, PS1, PUR	ATP (10 uM)	0.112	-16.571	Fail	-
7	MTNR1B	PVC1–3	MT (10 uM)	0.082	0.935	Pass	1.19×10^{-3}
8	MTNR1A	PVC1–3	MT (10 uM)	0.131	0.789	Fail	-
9	ADORA 1	PE1–3, PP1–2, PS1–2, PUR	NECA (10 uM)	0.354	-1.122	Pass	0.013
10	ADORA 1	PVC1–3	NECA (10 uM)	0.329	0.475	Pass	1.32×10^{-3}
11	MTNR1A	PVC1–3	MT (10 uM)	6.44×10^{-7}	0.111	Pass	5.44×10^{-4}
12	ADORA 1	PUR	NECA (30 uM)	0.409	-1.011	Pass	0.014
12	HTR2C		LSD (10 uM)	0.636	-5.701	Fail	-
12	HTR1A		LSD (10 uM)	0.941	-0.411	Pass	0.031
13	MTNR1A	PVC1–3	MT (10 uM)	7.72×10^{-6}	0.366	Pass	9.82×10^{-5}
14	ADORA 1	PE1–3, PP1–2, PS1–2, PUR, PVC1	NECA (50 uM)	0.354	-1.271	Pass	7.32×10^{-3}
15	HTR1A	PE1–3, PP1–2, PS1–2, PUR	LSD (10 uM)	0.381	-1.183	Pass	0.931
16	ADORA 1	PVC1–3, PUR	NECA (50 uM)	0.258	0.181	Pass	7.98×10^{-3}
17	HTR1A	PE1–3, PP1–2, PS1–2, PUR	LSD (10 uM)	0.395	-0.023	Pass	0.192
18	ADORA 1	PE1–3, PP1–2, PS1–2, PUR	NECA (50 uM)	0.439	-0.395	Pass	0.025
19	ADORA 1	PVC1–3	NECA (50 uM)	0.746	0.218	Pass	0.017
20	ADORA 1	PE1–3, PP1–2, PS1–2, PUR	NECA (50 uM)	0.354	0.198	Pass	0.011
21	ADORA 1	PVC1–3	NECA (50 uM)	0.281	0.404	Pass	0.019

3.2.2 Assay quality

A Z-factor was calculated to estimate the quality of the experiments based on the GPCR activation by the reference compound. Even though a Z-factor below 0 was not considered a failing factor of the experiments on its own, experiments with extremely low Z-factors (where EC_{50} values could not be calculated) were excluded. Of the 21 total experiments conducted, 6 of them had Z-factors > 0.5, 8 of them had Z-factors between 0.5 and 0, and 7 of them were below 0. Experiments 6 and 12 (HTR2C) had the lowest Z-factors (-16.571, and -5.701), neither of which were used to evaluate the GPCR activity of plastic extracts (Table 5).

3.2.3 Positive control concentration-response curve

A positive control concentration-response curve for each receptor studied in this thesis include MTNR1A, MTNR1B, HTR1A, HTR2C, and ADORA1 (Figure 8). Curves were visually inspected to check for sigmoid shape and accordingly categorized as pass or fail (Table 5). Experiments in which the reference compound did not produce a sigmoid concentration-response relationship were not used to evaluate receptor activation by plastic extracts. This applies to experiments 6, 8, and 12 (HTR2C).

3.2.3.1 Melatonin receptor 1A and 1B

MTNR1A transfected cells were exposed to melatonin as its reference compound. There were seven experiments including a positive control for MTNR1A (Figure 8A). Experiments 4, 11, and 13 were excluded to evaluate activity of plastic extracts due to failure in the Wilcoxon signed-rank test. Also, experiment 8 did not pass the criteria of a sigmoid shape and was for that reason excluded in this thesis. Experiment 1, 2, 3, 4, 11, and 13 all displayed sigmoid shaped curves indicating functioning reference compounds. Melatonin caused a maximum activation of 8.29-fold at MTNR1A. The remaining experiments that passed the three quality criteria were experiments 1, 2, and 3. These had EC_{50} values of 1.75×10^{-4}, 2.29×10^{-4}, and 1.64×10^{-4} µM and Z-factor values of 0.663, 0.708, and 0.408, respectively (Table 5).

MTNR1B was also exposed to melatonin to ensure proper receptor activation in experiments 3, 5, and 7 (Figure 8B). The three conducted experiments all indicated the same, well-functioning reference compound with a sigmoid curve, and melatonin caused a maximum activation of 38.58-fold at MTNR1B. Experiments 3, 5, and 7 were all considered in terms of

plastic extract receptor activation, and they had EC_{50} values of 3.75 x 10^{-3}, 2.61 x 10^{-3}, and 1.19 x 10^{-3} µM and acceptable Z-factor values of 0.371, 0.779, and 0.935, respectively (Table 5).

3.2.3.2 Serotonin receptor 1A and 2C

HTR1A was exposed to lysergic acid diethylamide (LSD) as a reference compound in three experiments. Experiments 12, 15, and 17 all indicated activation of the receptor because of the sigmoid curved graphs (Figure 8C), and LSD caused a maximum activation of 2.96-fold at HTR1A. The three HTR1A experiments had EC_{50} values of 0.031, 0.931, and 0.192 µM, respectively. Further, experiments 12, 15, and 17 had Z-factor values of -0.411, -1.183, and -0.023 (Table 5). Although the Z-factors are not considered critically low, the negative numbers still speak to a poorer quality of experiments compared to the melatonin experiments.

HTR2C was exposed to the same positive control as HTR1A, that is, LSD. This positive control did not result in a sigmoid concentration-response relationship in experiment 12 (Figure 8D). For that reason, in addition to the Z-factor being critically low at -5.701 (Table 5), the assay for this receptor did not work with LSD as a positive control and further experiments with this receptor were not conducted.

3.2.3.3 Adenosine receptor A_1

The reference compound for ADORA1 was 5′-N-ethylcarboxamide adenosine (NECA). The nine experiments with ADORA1 using NECA as reference compound were experiments 9, 10, 12, 14, 16, 18, 19, 20, and 21, all with acceptable sigmoid concentration-response curves (Figure 8E). After the first two of these experiments (9 and 10), the highest concentration of NECA was increased from 10 µM to 30 µM for experiment 12, and further increased to 50 µM for the remaining experiments to obtain a higher fold activation of the reference compound. NECA (50 µM) caused a maximum activation of 3.44-fold at ADORA1. Experiments 9, 10, and 12 were excluded due to cytotoxicity, inconsistencies in timing, and pipetting error, respectively. Experiments 14, 16, 18, 19, 20, and 21 had EC_{50} values of 7.32 x 10^{-3} µM, 7.98 x 10^{-3} µM, 0.025 µM, 0.017 µM, 0.011 µM, and 0.019 µM and Z-factor values of -1.271, 0.183, -0.395, 0.218, 0.198, and 0.404, respectively (Table 5).

Note that the cells in one ADORA1 experiment (experiment 6), before the nine mentioned experiments, were exposed to adenosine triphosphate (ATP) as reference compound (Appendix

D, Table D.1). This did not result in a sigmoidal concentration-response relationship, and it was therefore concluded to change the reference compound from ATP to NECA for ADORA1.

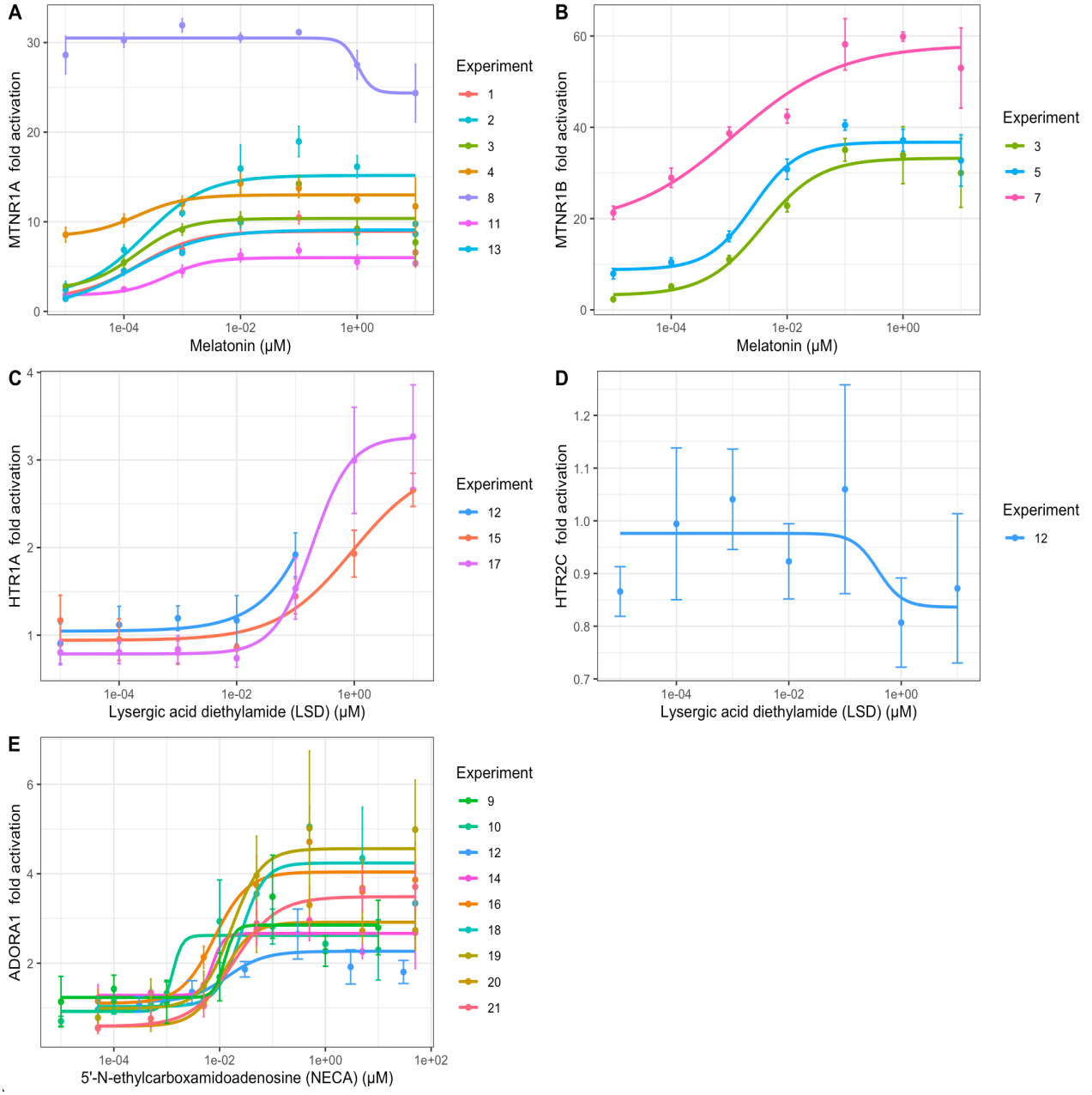

Figure 8: HTLA cells exposed to seven concentrations of their respective reference compound (n = 2–4). Note that the y axis of the subfigures are not scaled the same. **(A)** Melatonin receptor 1A (MTNR1A) exposed to melatonin. **(B)** Melatonin receptor 1B (MTNR1B) exposed to melatonin. **(C)** Serotonin receptor 1A (HTR1A) exposed to lysergic acid diethylamide (LSD). The two higher LSD concentrations of experiment 12 is not graphed due to luminescence overflow in the plate reader. **(D)** Serotonin receptor 2C (HTR2C) exposed to lysergic acid diethylamide (LSD). **(E)** Adenosine receptor A_1 (ADORA1) exposed to 5′-N-ethylcarboxamide adenosine (NECA).

3.2.4 Plastic extracts

The PRESTO-Tango assay was conducted to explore agonism of chemicals from eleven plastic samples on four GPCRs (Table 6). The concentration-response relationships for each receptor were constructed with seven concentrations of each plastic extract (Figure 9–11). Plastic extract causing activation above the LOD were considered to contain agonists of the receptor in question. EC_{50} values are presented for receptor-plastic extract interactions above the LOD. The positive control and plastic extract concentration-response curve of each individual PRESTO-Tango assay are provided in Appendix D (Table D.1).

Table 6: Overview of each receptor-plastic extract interaction. Each interaction is categorized as True/False based on whether the highest concentration of plastic extract treatment passed the limit of detection (LOD).

Receptor	Plastic extract	Activation	EC_{50} (mg plastic/well)
MTNR1A	PVC1	False	-
MTNR1A	PVC2	True	0.111
MTNR1A	PVC3	True	0.318
MTNR1B	PVC1	False	-
MTNR1B	PVC2	False	-
MTNR1B	PVC3	False	-
ADORA1	PE1	False	-
ADORA1	PE2	False	-
ADORA1	PE3	False	-
ADORA1	PP1	False	-
ADORA1	PP2	False	-
ADORA1	PS1	False	-
ADORA1	PS2	False	-
ADORA1	PUR	True	2.1×10^{-3}
ADORA1	PVC1	False	-
ADORA1	PVC2	True	1.558
ADORA1	PVC3	False	-
HTR1A	PE1	False	-
HTR1A	PE2	False	-
HTR1A	PE3	False	-
HTR1A	PP1	False	-
HTR1A	PP2	False	-
HTR1A	PS1	False	-
HTR1A	PS2	False	-
HTR1A	PUR	False	-

3.2.4.1 Melatonin receptor 1A and 1B

Both PVC 2 and PVC 3 activated the MTNR1A receptor (Figure 9A). The four highest concentrations of PVC 2 (0.225, 0.45, 0.9, and 1.8 mg plastic/well) and the three highest concentrations of PVC 3 (0.45, 0.9, and 1.8 mg plastic/well) activated the receptor over the

LOD. PVC 2 and PVC 3 activated MTNR1A at 36.16% and 25.29%, respectively, indicating that PVC 2 activation of the receptor was most effective. The EC_{50} values of the two PVC samples exposed to MTNR1A were 0.111 mg plastic/well for PVC 2 and 0.318 mg plastic/well for PVC 3 (Table 6), indicating that PVC 2 had the highest potency of the two.

None of the three PVC samples activated MTNR1B, and thus we conclude that none of the PVC samples contained chemicals that activated MTNR1B above the LOD (Figure 9B).

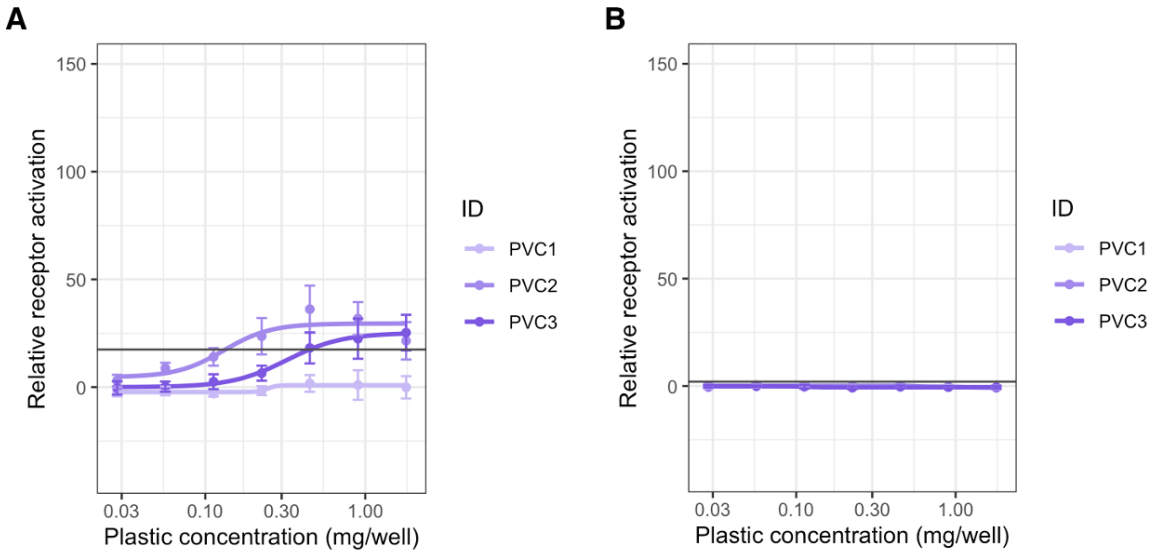

Figure 9: Melatonin receptors exposed to three PVC samples (n = 11–16). The grey, horizontal line in both subfigures illustrates the limit of detection (LOD). **(A)** Melatonin receptor 1A (MTNR1A). **(B)** Melatonin receptor 1B (MTNR1B).

3.2.4.2 Serotonin receptor 1A

None of the plastic extracts caused activity of HTR1A over the LOD. However, PS 1 showed a trend towards a slight activation (18.99%) in a concentration-dependent manner (Figure 10C). This indicates that there may be weak partial agonists in the plastic extracts.

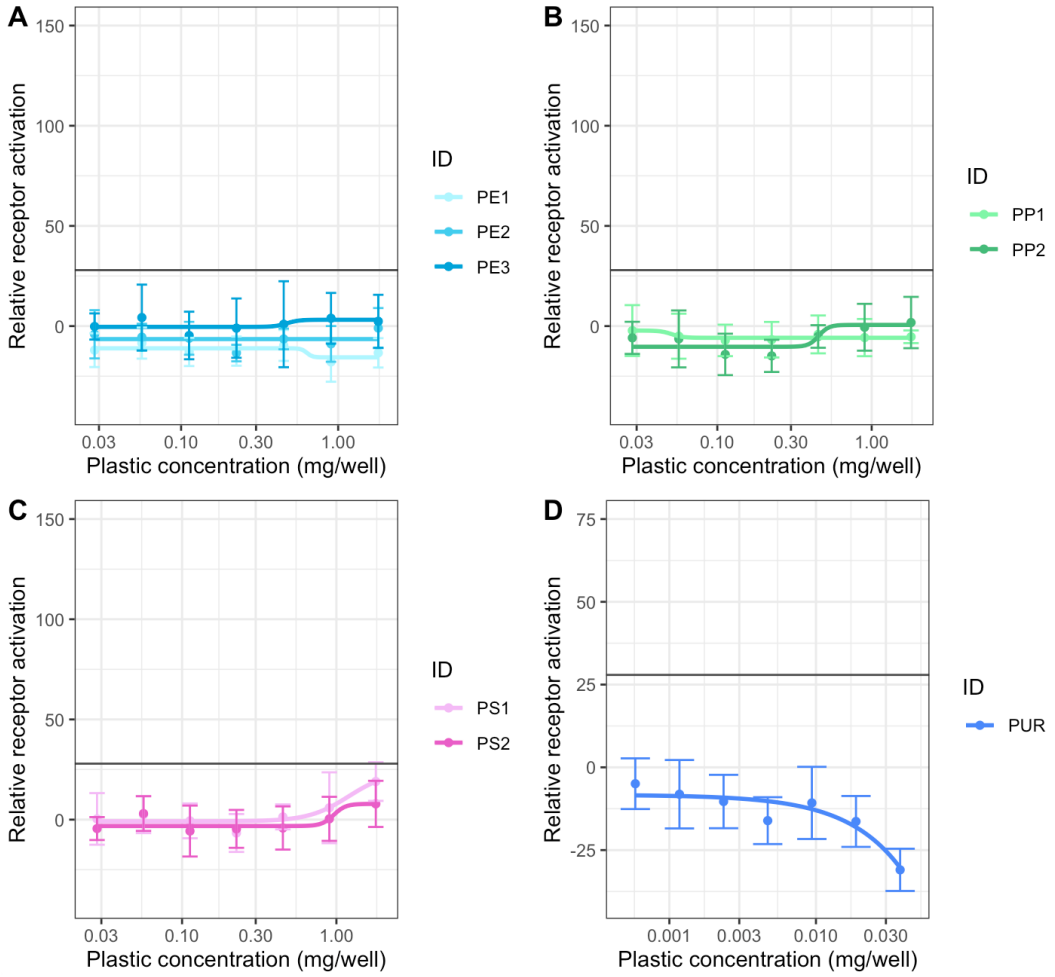

Figure 10: Serotonin receptor 1A (HTR1A) exposed to four plastic polymer types (n = 6–8). The grey, horizontal line in each subfigure illustrates the limit of detection (LOD). **(A)** Polyethylene (PE). **(B)** Polypropylene (PP). **(C)** Polystyrene (PS). **(D)** Polyurethane (PUR).

3.2.4.3 Adenosine receptor A_1

The five highest concentrations of PUR (2.34 x 10^{-3}, 4.69 x 10^{-3}, 9.38 x 10^{-3}, 1.88 x 10^{-2}, and 3.75 x 10^{-2} mg plastic/well) caused activation of the receptor above the LOD (Figure 11D). Note that the concentrations of PUR are 48 times lower than for the other plastic extracts. PUR activation of ADORA1 had an EC_{50} of 2.1 x 10^{-3} mg plastic/well (Table 6). The highest concentration of PVC 2 (1.8 mg plastic/well) also caused activation above the LOD for ADORA1 and had an EC_{50} of 1.558 mg plastic/well (Figure 11E). PUR and PVC 2 caused activation of ADORA at 100.21% and 48.43%, respectively, indicating that agonism by chemicals in PUR was more effective. Further, PUR was clearly the most potent of the two plastic samples because of the much lower EC_{50} value.

None of the other polymer types (PE, PP, or PS) activated ADORA1. However, though not above the LOD, PP 1 caused slight activation (31.28%) in a concentration-dependent manner, indicating the possible presence of weak partial agonists. Similarly, PVC 1 and PVC 3, caused slight activation of 9.01% and 20.16%, respectively.

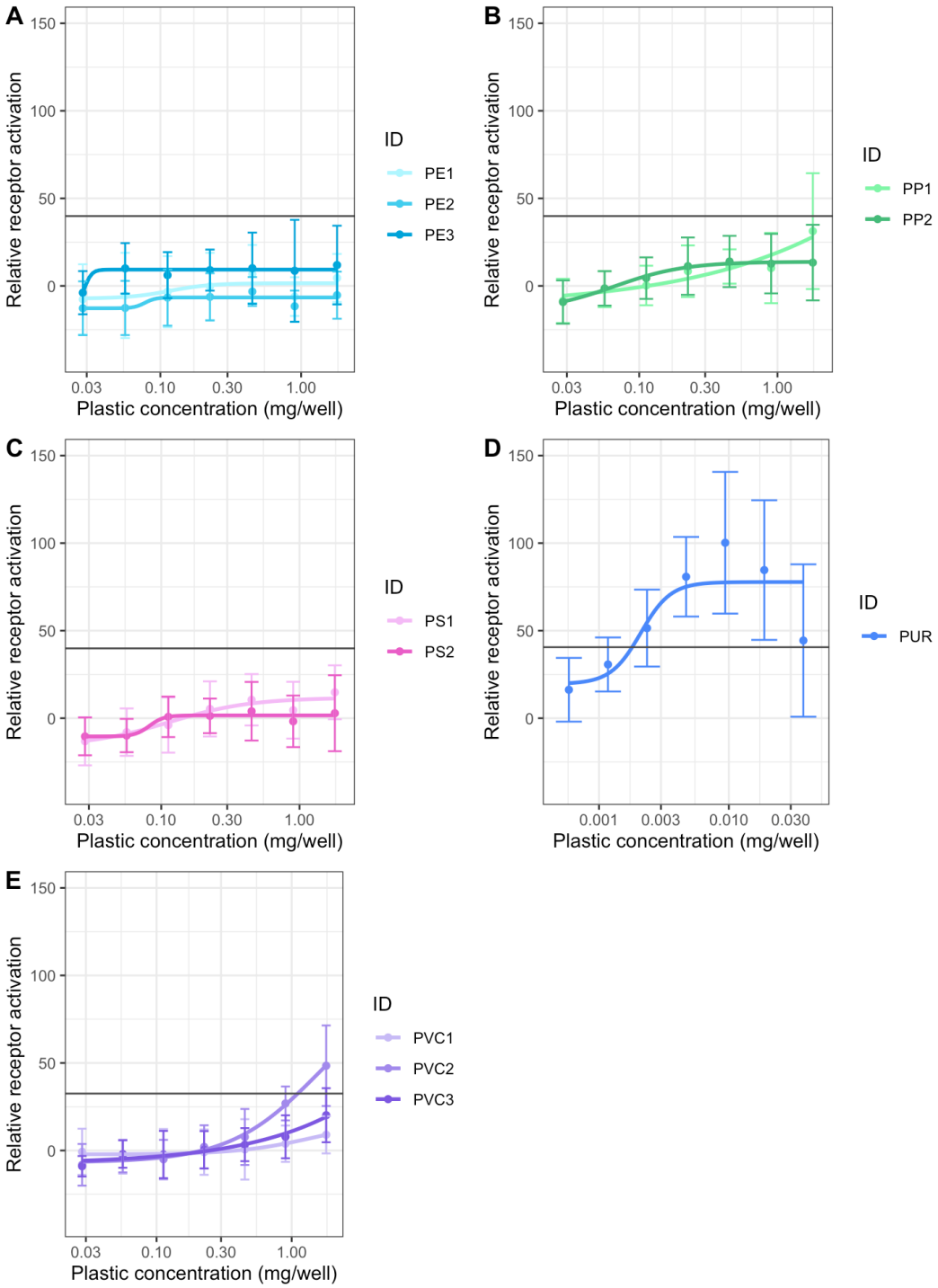

Figure 11: Adenosine receptor A_1 (ADORA1) exposed to five plastic polymer types (n = 9–16). Note that the X axis of subfigure D differs from the others. The grey, horizontal line in each subfigure illustrates the limit of detection (LOD). **(A)** Polyethylene (PE). **(B)** Polypropylene (PP). **(C)** Polystyrene (PS). **(D)** Polyurethane (PUR). **(E)** Polyvinyl chloride (PVC).

3.3 Chemical analysis

Clustering analyses for both polymer mixes provide insight into similarities and differences between the chemical composition of the PE, PP, PS, PUR, and PVC samples. The chemical features in active samples were filtered against the inactive ones to reduce the number of chemical features and therefore suggest potential agonists of the respective GPCRs (Table 7). Additionally, features with particularly high abundance are suggested as agonists (Table 8 and Table 9).

Table 7. Number of features for each active plastic sample, and the number of possible agonists after filtering steps resulting in number of features with a fold change to the inactive samples of the polymer mix ≥ 5.

Sample	Number of features	Number of possible agonists
PVC2	3274	472
PVC3	2332	550
PUR	4007	2279

3.3.1 PVC mix

Dendrograms show that PVC 2 and PVC 3 are clustered together indicating that they are similar and share more chemical features than with PVC 1 (Figure 12). This is also shown by the color scheme of the two samples being similar, with lower abundancies in PVC 2 and PVC 3. Chemicals from PVC 2 activated both MTNR1A and ADORA1, and chemicals from PVC 3 activated MTNR1A.

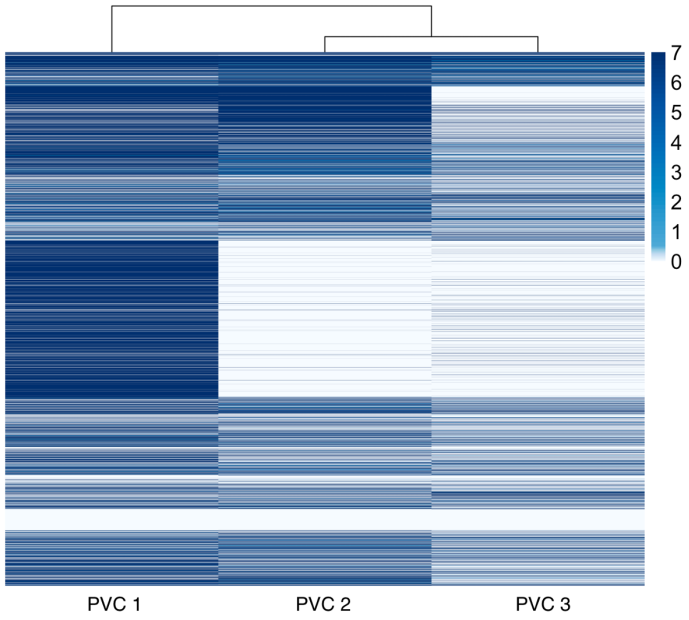

Figure 12: Heatmap illustrating chemical composition and similarities of three PVC samples. Darker color indicates higher abundance of the feature. Dendrograms denote the clustering between plastic samples.

There were 3274 features present in PVC 2 and 2332 features present in PVC 3 (Table 7). Features that were at least five times more abundant in the active sample than the inactive sample were considered candidates that may activate MTNR1A and ADORA1, thereby reducing the list of possible agonists to 472 features for PVC 2 (85.6% reduction) and 550 features for PVC 3 (76.4% reduction). Of these possible agonists, the 10 most likely features to be responsible for the agonism were selected based on their high abundance in the plastic extract (Table 8). For PVC 2, the feature with the highest abundance had 208684.97 ion counts with a fold change of 6.61 compared to the PB, indicating a FCA with numerous plastic chemicals. The same was indicated for PVC 3 where the feature with the highest abundance had 40778.63 ion counts with a fold change of 763.66 compared to the PB.

Table 8: Top 10 list of likely agonists for PVC 2 and PVC 3. The list includes the compound name given in mass per charge (feature), the intensity of the feature peak (feature abundance), and the fold change compared to the inactive compounds of the PVC mix. Where fold change is absent, the given feature was not present in the inactive samples.

Sample	Feature	Feature abundance	Fold change
PVC2	31.39_1010.6687 n	208684.97	6.61
	31.19_1011.6760 m/z	72777.29	5.12
	28.40_604.3157 m/z	57862.73	-
	31.18_424.3730 n	54293.74	5.18
	30.80_1029.6779 m/z	31475.59	10.55
	30.89_687.4807 m/z	28510.37	23.38
	34.29_1183.9645 m/z	25916.19	-
	33.10_657.6150 m/z	20837.74	10.97
	28.40_596.3265 m/z	13553.46	27.29
	35.69_675.5163 m/z	13165.99	5.13
PVC3	24.95_309.2042 m/z	40778.63	763.66
	35.84_359.2941 m/z	29751.47	-
	35.98_409.3069 m/z	13237.91	197.02
	27.85_604.3153 m/z	10829.21	3087.31
	32.15_647.9444 m/z	6754.15	5.83
	29.09_330.2767 n	5808.28	32.42
	30.20_295.1943 m/z	5721.62	35.24
	31.01_885.7889 m/z	5308.32	9.97
	23.44_301.1411 m/z	5187.73	5.61
	27.00_419.2737 m/z	5132.12	64.49

3.3.2 Diverse polymer mix

PUR is most dissimilar to the other samples in the diverse polymer mix. There is no apparent grouping of polymer types based on their chemical features (Figure 13), thereby indicating unique chemical profiles for each product as opposed to each polymer type. Only chemicals from PUR activated ADORA 1, however PP1 also showed weak activity below the LOD.

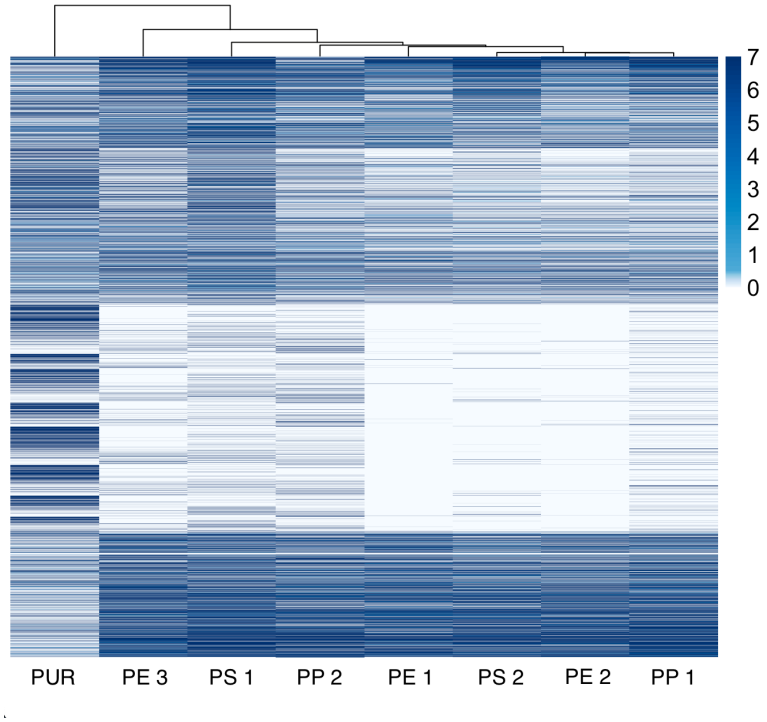

Figure 13: Heatmap illustrating chemical composition and similarities of three PVC samples. Darker color indicates higher abundance of the feature. Dendrograms denote the clustering between plastic samples.

There were 4007 features in PUR (Table 7). Features that were at least five times more abundant in the active sample than the inactive sample were filtered out and considered candidates that may activate ADORA1. After the filtering steps, the list of possible agonists was reduced to 2279 (43.2% reduction). The 10 most likely features to be responsible for the agonism were selected based on their high abundance in the plastic extract (Table 9). The feature with the highest abundance had 527222.95 ion counts with a fold change of 62642.19 compared to the PB. This indicates a FCA constituting of numerous plastic chemicals.

Table 9: Top 10 list of likely agonists for PUR. The list includes the compound name given in mass per charge (feature), the intensity of the feature peak (feature abundance), and the fold change compared to the inactive compounds of the PVC mix. Where fold change is absent, the given feature was not present in the inactive samples.

Sample	Feature	Feature abundance	Fold change
PUR	24.82_326.0717 n	527222.95	62642.19
	34.13_324.2079 m/z	524810.74	7234595.34
	28.03_455.3353 m/z	462267.19	195182.87
	29.51_527.3926 m/z	445705.49	-
	32.21_648.5194 n	443084.89	4842.27
	32.86_360.2885 n	404736.09	1745.34
	30.85_599.4509 m/z	396889.64	74838.88
	33.54_792.6344 n	352478.78	-
	25.72_383.2771 m/z	325850.22	227745.30
	26.06_365.1361 m/z	274245.14	645.26

4. Discussion

This study investigated the potential agonism on five GPCRs (MTNR1A, MTNR1B, HTR1A, HTR2C, and ADORA1) by plastic extracts of five polymer types from FCAs (PE, PP, PS, PUR, and PVC). The study involved cytotoxicity testing, PRESTO-Tango bioassays, and non-target chemical analysis to combine research on cytotoxicity, receptor activation, and the chemical composition of the activating plastic extracts. This allowed for an in-depth investigation on plastic chemicals of unknown hazard. The major finding of this project was that chemicals in PVC and PUR activated MTNR1A and ADORA1. To our knowledge, this is the first study exploring agonism by plastic chemicals on the five investigated receptors. The results of this study provide valuable insight into the cytotoxicity of the five plastic polymer types and their mixture toxicity. We identified novel receptors and unique modes of action by which chemicals present in food packaging are disrupting cellular signaling.

4.1 Cytotoxicity testing

Cytotoxicity testing was performed to investigate possible toxic effects of the individual polymer extracts and mixtures on HTLA cells. This was done to ensure that HTLA cells were not exposed to cytotoxic concentrations of plastic extracts in the PRESTO-Tango assay, and further, to explore the differences in cytotoxicity caused by polymer mixes and individual samples. Of the 11 individual polymer samples and 2 polymer mixes investigated in this thesis, PUR contained chemicals that induced the most cytotoxicity of the polymer types. PUR induced cytotoxicity with the highest non-cytotoxic concentration (HNC) being 0.038 mg plastic/well (Table 4). This result is supported by toxicity hits on AREc32 cells (Zimmermann et al., 2019), CALUX cells (Völker et al., 2022), and various aquatic invertebrates (Lithner et al., 2009, Bejgarn et al., 2015, Li et al., 2016), who also found PUR to be more toxic than other polymer types. PUR is characterized by large numbers and quantities of chemicals, and further, PUR is considered highly hazardous based on chemical composition compared to other plastic polymers (Lithner et al., 2011). For that reason, our results conform with the literature. Further, 10 of the 12 remaining plastic samples were cytotoxic with a HNC at 4.5 mg plastic/well. For most of the sample's chemicals to be cytotoxic at this concentration was somewhat expected as cytotoxicity by some of these polymer types previously have been induced by considerably lower concentrations. For instance, two PUR samples and one PP sample were cytotoxic in CALUX cells at 3 mg plastic/well (Völker et al., 2022), and three PUR samples and one PS sample were cytotoxic in AREc32 cells at > 1.88 mg plastic (Zimmermann et al., 2019). The

cytotoxicity hits observed in this study showed that the PUR sample contained chemicals that induced higher cytotoxicity than the other polymer types, and that most of the FCAs contained chemicals that caused cytotoxicity on HTLA cells at 9 mg plastic/well.

In addition to investigating individual polymer samples, we also explored the cytotoxicity of polymer mixtures. Treatment with the PVC mix in this study resulted in cell counts lower than for any of the individual PVC extracts constituting the mix (Figure 7). The individual plastic samples are diluted in the mixtures, and thus, the concentration of each sample is lower as a constituent of either the diverse polymer mix or the PVC mix. The mixture effect is apparent in the PVC mix as the EC_{20} values is lower than the three PVC extracts, despite the concentration of each individual sample being lower in the mixture. This shows that the mixture toxicity was higher than for the individual samples, and thus, none of the individual samples caused the total cytotoxicity effect of the mix. However, the same effect was not observed in the diverse polymer mix. This was likely due to the high cytotoxicity of PUR. This sample, even when being 60 times less concentrated compared to the other plastic extracts, had a lower EC_{20} than the mixture. As PUR induces strong cytotoxicity, the effect of the diverse polymer mix was likely caused by this sample.

The mixture effect observed in this thesis is concerning as toxic effects can be observed in a mixture even if the individual substances alone does not cause a significant effect (Kortenkamp et al., 2007), and further, the overall mixture effect can exceed individual substance effects (Grob et al., 2006). Mixture effects are highly problematic as risk assessments focus on starting substances of plastics, and not the effect of the final plastic product (Muncke et al., 2020). Moreover, there are no general regulations or uncertainty factors regarding mixture effects, and thus, the potential threats of mixtures are not accounted for despite being a well-described phenomenon (Kortenkamp and Faust, 2018, Muncke et al., 2020). The challenges regarding plastic mixture effects are clear, and because humans are exposed to mostly mixtures of plastic polymer types and chemicals through FCMs, it is crucial to unravel and account for these effects to exclude potential threats to human health (Muncke et al., 2017).

4.2 Positive controls as quality assurance

This study investigated five receptors (MTNR1A, MTNR1B, HTR1A, HTR2C, and ADORA1), and a reference compound was included for each of these. Confirmation of

activation by a reference compound is important to establish and ensure the function of the receptor (vom Saal and Welshons, 2006). A functioning reference compound-receptor interaction was obtained for four of the five receptors (MTNR1A, MTNR1B, HTR1A, and ADORA1, Figure 8). This means that the reference compound had sufficient affinity (receptor binding) and efficacy (receptor activation) to bind to and activate the receptor (Strange, 2008), and shows that the assay is working with these receptors. As a result, these experiments were validated by the positive control and, thus, passed this quality criterion.

Activation of both MTNR1A and MTNR1B by the reference compound melatonin was used to validate that the PRESTO-Tango assay worked with these receptors. Consequently, assays involving these receptors (that also met the other quality criteria) were accepted as measures of plastic activation. Even though both receptors were activated by the same reference compound, their potency and efficacy were not the same. The potency represented by the EC_{50} value is higher for MTNR1A than for MTNR1B (Figure 8A–B). This indicates that reference compound has a higher affinity for the former. Melatonin does have a slightly higher affinity to MTNR1A than to MTNR1B (Hardeland, 2012b), and for that reason, our results did not conform with the literature. However, the fold activation of melatonin is 4.65 times higher for MTNR1B than MTNR1A, suggesting that the efficacy is higher for MTNR1B in this study. On the contrary, similar research found that melatonin had a higher efficacy at MTNR1A than at MTNR1B (Kroeze et al., 2015). The opposite observations in this study could be an artifact of the assay, meaning a result that does not represent the true biological function caused by technical (and often artificial) processes (Coussens et al., 2004). A potential artifact could be that transfection of HTLA cells with MTNR1B worked better, and thus, resulted in cell surface expression of more receptors than what was the case for MTNR1A. Nevertheless, melatonin was concluded to be a successful reference compound for both melatonin receptors in this study.

Treatment of HTR1A with LSD resulted in a sigmoidal concentration-response curve, indicating a functioning reference compound and assay (Figure 8C). For that reason, assays with HTR1A that also passed the other quality criteria were accepted as measures of plastic chemical receptor activation. LSD is a partial agonist of HTR1A (Janowsky et al., 2014), for that reason we expected it to activate the receptor. In contrast, HTR2C was excluded from this thesis because LSD treatment did not result in a proper concentration-response relationship (Figure 8D). In similar research, HTR1A and HTR2C have been exposed to different ligands to obtain functioning positive controls (Kroeze et al., 2015). As in this study, HTR1A activation

by LSD as reference compound was successful, but for HTR2C, serotonin (5-HT) is reported as reference compound. This indicates that similar research could not obtain a proper concentration-response relationship for HTR2C using LSD as a reference compound. This shows that HTR1A and HTR2C are not necessarily activated by the same ligands as observed in this study. To conclude, LSD was accepted as reference compound for HTR1A, but not for HTR2C, and consequently, further HTR2C experiments were not conducted.

Positive control concentration-response curves were obtained for NECA at ADORA1 (Figure 8E). This outcome was in line with the literature as NECA is a highly potent agonist of ADORA1 (Bhalla et al., 2020). Activation of the receptor by NECA has been successful in similar research (Kroeze et al., 2015), emphasizing the function as reference compound for this receptor. Because of availability, ATP was attempted as a reference compound in one experiment for ADORA1 (Table D.1). However, this did not result in sigmoid shaped concentration-response curve. As similar research also found that ATP could not be validated as reference compound (Kroeze et al., 2015), ATP was disclosed as a non-functioning reference compound in this study. NECA, however, successfully activated ADORA1, and was accepted as reference compound.

Activation of GPCRs is dependent on two aspects: the affinity of the ligand, that is the ability to bind to the receptor, and the efficacy, that is the ability to affect the receptor leading to an effect of the associated signaling systems (Strange, 2008). Accordingly, lower affinity and correspondingly higher EC_{50} values indicates poorer binding between the ligand and the receptor, while higher efficacy and followingly higher fold changes indicates strong receptor activation by the ligand. It is noteworthy that high affinity of ligand-receptor interactions does not necessary result in high efficacy, i.e., highly potent ligands could induce low receptor effects. Although the same assay was used for each receptor in this study, varying potency and fold activation was observed for the different reference compound-receptor interactions. Overall, it is apparent that melatonin had the highest affinity and efficacy on the melatonin receptors, followed by NECA's activation of ADORA1, and least affinitive and effective was LSD's activation of HTR1A. These differences could be caused by varying success of receptor transfection. Transfection efficiency is dependent on various factors such as health and viability of the cell line, degree of cell confluency, plasmid quality, and number of passages. Poorer transfection of receptors could lead to fewer expressed receptors and accordingly, lower receptor response (Kim and Eberwine, 2010, ThermoFisher Scientific, 2022). Differences could

also be caused by artifacts such as interference of test compounds and assay reagents or biological molecules (Dahlin et al., 2015). However, for substances to bind to receptors with varying affinity and efficacy is a natural phenomenon (Chen et al., 2017). Different ligand-receptor interaction effects have also been observed in similar research (Kroeze et al., 2015), and thus, variety of receptor effects are in line with the literature.

To summarize, the quality assurance regarding reference compound-receptor interactions resulted in acceptance of MTNR1A, MTNR1B, HTR1A, and ADORA1 as measures of plastic chemical activation. A functioning reference compound was not found for HTR2C, and thus, this receptor was not further investigated in this thesis.

4.3 PRESTO-Tango assay

4.3.1 Melatonin receptor 1A and 1B

The PRESTO-Tango assay was performed to investigate agonism by plastic extracts obtained from FCMs on the MTNR1A, MTNR1B, HTR1A, and ADORA1 receptors. The PRESTO-Tango analysis showed that two out of three PVC samples included in this study activated MTNR1A (Figure 9A). On the basis of previous hits of the PVC activating MTNR1A (McPartland et al., 2022), the result of one or more of the PVC extracts inducing receptor activation conform with the literature. To our knowledge, MTNR1A agonism by specific plastic polymer types has not been studied prior to this thesis. However, highly toxic pesticides have activated MTNR1A. Both carbaryl and carbofuran are MTNR1A activating (Popovska-Gorevski et al., 2017, Glatfelter et al., 2021), further confirming that synthetic chemicals can disrupt MTNR1A. Further, previous research show that di-(2-ethylhexyl) phthalates (DEHP) have changed MTNR1A gene expression in rodents (Gao et al., 2018). Although direct receptor activation by DEHP was not explored, the treatment of this chemical to pregnant rats resulted in down regulation of the MTNR1A gene in newborn rats due to the prenatal exposure. This show that plastic chemicals have affected MTNR1A in mammals and emphasizes the importance of investigating MTNR1A disruption in humans as well.

While two PVC samples activated MTNR1A, one PVC sample did not cause agonism. Although all three samples are classified as PVCs, PVC 1 did not induce receptor activation. This emphasizes that the polymer type is not the direct cause of receptor activation, but rather the chemical compositions of the plastic samples. Even though the two activating PVC FCAs had similar purpose, PVC 2 and PVC 3 were extracted from different FCAs, namely a drinking tube and a drinking bladder tube, respectively. This shows that it may not make a difference for us as consumers to avoid specific polymer types, and thus, that the consumer cannot take precautions regarding FCC risk based on polymer type alone.

Interestingly, none of the PVC samples activated MTNR1B (Figure 9B). Previous work on the two melatonin receptors resulted in the PVC mix only activating MTNR1A (McPartland et al., 2022), and thus, this result conform with the literature. Although the two melatonin receptors are both important regulators of the circadian rhythm, the receptors play different roles in the regulation of the day/night phase shift, with MTNR1A inhibiting neuronal activity and MTNR1B phase shifting circadian firing rhythms (Dubocovich, 2007). MTNR1A and MTNR1B agonists are often described as activating on both melatonin receptors (Laudon and Frydman-Marom, 2014), but several agonists show significantly higher affinity for either one of the them (Dubocovich et al., 1997). This indicates the likelihood of the plastic chemicals having different affinities for the two receptors, and thus, indicates that plastic chemical agonism can favor one receptor over another despite having the same natural ligand.

The agonism observed at MTNR1A suggests that FCCs could disrupt the melatonin signaling pathway. Although this thesis shows that plastic chemicals activate MTNR1A expressed by HTLA cells, the consequence of such GPCR disruption in an organism is yet to be investigated. Known melatonin receptor agonists are therapeutical compounds available for treatment of insomnia, depression, and circadian rhythms sleep-wake disorders (Laudon and Frydman-Marom, 2014). This thesis demonstrates the potential of plastic chemicals to imitate MTNTR1A agonists potentially effecting receptor stimulation in otherwise healthy people, and result in undesirable stimulation and unfavorable consequences. However, the affinity and efficacy of agonists highly vary, and the physiological effect of agonists does not necessarily imitate the natural ligand of the receptor even at maximum receptor occupancy (Waldman, 2009). Nevertheless, melatonin signaling disruption is linked to various conditions and diseases such as dementia, mood disorders, and diabetes type 2 (Hardeland, 2012a), and thus, GPCR

disruption of MTNR1A by FCCs could have critical human health effects and therefore warrants further investigation.

4.3.2 Serotonin receptor 1A

HTR1A was included in this thesis because of previous research demonstrated a change in transcript levels caused by BPA (Castro et al., 2015). However, none of the plastic samples constituting the diverse polymer mix caused activation of HTR1A receptor (Figure 10). Possible explanations could be that HTR1A agonists are simply not present in the samples. Conversely, it could also be due to the presence of antagonists or inverse agonists canceling out potential agonist activity (Sum et al., 2019). This could explain the slight activation of PS 1 observed ((Figure 10C). Within the ToxCast dataset there are three assays reporting > 70 HTR1A activating compounds (Environmental Protection Agency, 2022), although, none of the reported agonists were known to be used in plastic chemicals. As demonstrated, plastic samples of the same polymer type can have large diversity in chemical and physical properties due to their varying chemical composition (Groh et al., 2019, Sridharan et al., 2022). Thus, the result of no HTR1A activation by the plastic samples investigated in this thesis does not exclude potential agonism by other plastic samples of the same polymer types.

4.3.3 Adenosine receptor A_1

In this study, PUR and one PVC sample activated ADORA1 (Figure 11), indicating that these FCAs contain chemicals that can disrupt ADORA1 signaling. Previous research on the diverse polymer mix and the PVC mix resulted in activation of ADORA1 by both mixes, and thus, the results of one or more plastic samples constituting the mixes to induce receptor activation conform with the literature (McPartland et al., 2022). Searching ToxCast for agonists of ADORA1 resulted in hits from three assays reporting > 100 ADORA1 activating compounds (Environmental Protection Agency, 2022). Among the compounds were BPA and phthalates, two known hazardous plastic chemicals that has been previously identified in PVC samples (Baralic et al., 2020, Skåland, 2022). Both of these chemicals possess GPCR disrupting properties, specifically for the estrogen binding G protein receptor 30 (GPC30) and ADORA1, and have unfavorable health effects in humans (Darbre, 2020, Environmental Protection Agency, 2022). Except for the two plastic samples containing ADORA1 agonists, none of the nine other plastic samples resulted in receptor activation. This indicates that none of the plastic

chemicals constituting these plastic samples had the affinity and/or the efficacy to result in receptor activation above the LOD.

The agonism caused by PUR and PVC chemicals observed at ADORA1 suggests that FCCs could disrupt adenosine signaling. Despite the effects of such agonism in an organism is yet to be investigated, this thesis demonstrate disruption of ADORA1 signaling for HTLA cells transfected with this receptor. Disruption in adenosine signaling pathways is of concern because of its important therapeutic role throughout most organ systems (Layland et al., 2014, Borea et al., 2018). Specifically, non-functioning adenosine signaling is linked to various cardiac diseases in addition to mood disorders and stroke (Layland et al., 2014). Accordingly, disruption of ADORA1 signaling pathways by FCCs of unknown physiological impact could have severe health effects.

To summarize, the findings from this work show that GPCRs are relevant targets of FCCs. Specifically, MTNR1A and ADORA1 are activated by FCCs, and further, PUR and PVC are the polymer types that contained the most GPCR agonists.

4.4 Chemical analysis

Non-target chemical analysis was performed to obtain a better understanding of the chemical composition of the FCAs investigated in this thesis. From the PRESTO-Tango analysis, PUR, PVC 2, and PVC 3 induced receptor activation. PUR and PVC are considered highly hazardous, and both polymer types are known to contain numerous plastic chemicals (Lithner et al., 2011). This is in agreement with the results of this study illustrating that PUR contained noticeably more chemical features than the other polymer types in the diverse polymers mix (Figure 13). Additionally, the grouping of PVC 2 and PVC 3 is reflected in their activity on the ADORA1 and MTNR1A receptors, indicating that these samples shared more chemical features than they did to PVC 1 (Figure 12). This work supports previous reports of PUR and PVC chemicals activating receptors. For instance, research on plastic exposure to the human estrogen receptor α (hERα) found that chemicals in several PUR and PVC samples caused agonism at this receptor (Zimmermann et al., 2019). Further, chemicals from PVC samples have activated the peroxisome proliferator-activated receptor gamma (PPARγ, Völker et al., 2022, Chen et al., 2022). Although both hERα and PPARγ are nuclear receptors, such activation indicates that plastic chemicals from PVC and PUR have the ability to interact with human cellular receptors.

In addition, this thesis showed that the same FCAs, namely PVC2, activated both ADORA1 and MTNR1A. This shows that one FCA can contain chemicals that disrupt multiple signaling processes and is concerning as this leaves the FCA more detrimental than what it would be if only one receptor was activated.

Although identification of chemical compounds was not a focus of this thesis, similar research have identified organophosphates and phthalates, both related to health concerns, as prevalent toxic chemicals in biologically active PVC samples (Chen et al., 2022). This underlines the importance of chemical analysis of plastic extracts and potential identification substances of concern. However, numerous chemicals in plastic products cannot be identified. For example, 14.4% and 15.7% of the PVC 2 and PVC 3 features, respectively, were identified from the non-target analysis conducted by our group, whereas 11.7% of the PUR features were identified (Skåland, 2022). A similar study identify as few as 8% of plastic chemicals in an overall sample (Zimmermann et al., 2021). This highlights the knowledge gap regarding the chemical composition of plastics. The list of possible agonists shows that hundreds of potential agonists for the PVC samples and thousands of possible agonists for PUR are unidentified (Table 7). This is highly problematic as a potential threat to human health cannot be established unless the chemical compounds constituting plastics are known (Muncke et al., 2020). However, this thesis demonstrated that the number of agonist candidates can be considerably narrowed down. Through filtering steps and comparison between active and inactive plastic samples, the inactive FCCs can be excluded, and thus, the list of possible agonists is shorter and more manageable. Further, this thesis shows that the top ten features of PVC 2 and PVC 3 are unique, indicating that the two samples do not share potential agonists. This emphasizes both the need for and challenges of establishing a better regulatory system regarding plastic chemicals in FCMs.

4.5 Limitations

In this work we have identified chemicals from one PUR and two PVC samples as agonists for MTNR1A and ADORA1. As most research, this study faced some challenges and limitations. Specific for this work was experiments that indicated solvent effect or had poorer quality. Within the cytotoxicity experiments the solvent showed a slight overall proliferative effect rather than a cytotoxic effect (Figure 7). The highest DMSO concentration in these experiments were 1.02%, and as this concentration could possibly cause cell viability reduction (de Abreu

Costa et al., 2017, Singh et al., 2017), a proliferative effect was not conforming with the literature. Previous research on FCCs also used DMSO as solvent, and they did not see any effect of the solvent (Zimmermann et al., 2019). For that reason, the placement of the negative control to the far right of the plate may have caused lower cell counts due to edge effect (Mansoury et al., 2021).

Further, three PRESTO-Tango assays were not accepted as measures of FCC agonism because of p values < 0.05 from the Wilcoxon test indicating a solvent effect. This applies to experiments 4, 11, and 13 (Table 5), and they had in common that they were the later MTNR1A involving experiments. For that reason, melatonin contamination of the solvent (DMSO) was suspected as a likely cause of this effect. As mentioned, previous research on FCCs did not see a solvent effect by DMSO (Zimmermann et al., 2019). Moreover, the highest DMSO concentration in the PRESTO-Tango assay were at 0.2% in this study, and thus, was within acceptable limits (Du et al., 2006, de Abreu Costa et al., 2017). This emphasizes that the apparent solvent effect was likely not caused by the solvent itself, but rather technical errors. Additionally, as for the cytotoxicity experiments, the placement of the negative to the far right of the plate may have caused lower cell counts due to an edge effect (Mansoury et al., 2021).

Lastly, experiments 6 and 12 of the PRESTO-Tango experiments were categorized as of critically poor quality due to low Z-factors (Table 5). These were consequently not accepted as measures of FCC agonism. Despite being a widely accepted standard measure on quality control (Zhang et al., 1999), the Z-factor has limitations such as being sensitive to lower efficacies that would cause lower Z-factor values (Birmingham et al., 2009). Technical errors affecting the HTLA cells, such as pipetting mistakes, could also cause higher standard deviation in negative and positive controls, and thus, effect the Z-factor.

In a larger context, it is important to note the limited sample size of this study. Although our results offer novel insight into signal disruption by FCCs to GPCRs, given the diversity of plastics, 13 plastic samples analyzed in this thesis are not representative for all FCAs (Zimmermann et al., 2019). Further, the extraction of the plastic samples does not represent chemicals that migrate under normal use conditions. Interestingly, research on the effect of plastics leaching in water showed toxicity and receptor activation (Zimmermann et al., 2021). However, being extracted in methanol in this study, the plastic extracts does not offer a realistic representation for consumers. Also, in the search for agonists of the receptors studied in this

thesis, it is to be noted that the ToxCast dataset might be limited in the coverage of chemicals, and especially for NIAS. The dataset might also be prone to false negatives and positives (Zimmermann et al., 2019). Another limitation to mention is artifacts of the assay in this study, such as luciferase inhibition, that could lead to false negatives (Auld and Inglese, 2016). Lastly, it should be noted that although being a unique and highly useful resource for interrogation of GPCR activation (Kroeze et al., 2015), we experienced that the PRESTO-Tango assay was not particularly stable in this study. By looking at the variation in positive controls of each receptor (Figure 8), we see variability between experiments with the same GPCR, and thus, this instability could be a source of variable GPCR response.

5. Conclusion and future research

This thesis investigated potential agonism by FCCs on five polymer types (PE, PP, PS, PUR, and PVC) to five GPCRs (MTNR1A, MTNR1B, HTR1A, HTR2C, and ADORA1). We treated HTLA cells with extracted plastic samples in cytotoxicity experiment and further, exposed the plastic samples to GPCRs transfected HTLA cells in PRESTO-Tango assays to investigate chemical agonism. The chemicals detected in the active plastic samples were analyzed and filtered to narrow down the list of possible agonists.

Cytotoxicity testing showed that PUR was by far the most cytotoxic plastic sample with the HNC being 0.038 mg/well. Although at higher concentrations, at least one sample of each polymer type induced cytotoxicity with a HNC of 4.5 mg/well. Further, there was a mixture effect of the PVC mix as the EC_{20} was noticeably lower than that of individual PVC samples constituting the mixture.

The PRESTO-Tango assay included a positive control as quality measure to assure the assay is working. Melatonin, LSD, and NECA was used as reference compounds for the melatonin receptors, serotonin receptor, and adenosine receptor, respectively. MTNR1A, MTNR1B, HTR1A, and ADORA1 were activated by their reference compound, demonstrating that the PRESTO-Tango assay was working properly for these receptors. HTR2C was not activated by the reference compound and was discontinued.

From the PRESTO-Tango assay, plastic chemicals from two PVC samples activated MTNR1A. This was hypothesized and in agreement with previous findings from our group. To our knowledge, plastic chemicals have not been reported as MTNR1A agonists in the literature. However, certain carbamate pesticides activate the receptor and phthalates downregulate the receptor gene. As melatonin signaling inefficiencies is linked to diseases, such as dementia, mood disorders, and diabetes type 2, MTNR1A disruption by FCCs could have critical human health effects. Further, one PVC sample and the PUR sample contained plastic chemicals that were ADORA1 agonists, also in accordance with the hypotheses. BPA and phthalates are plastic chemicals that have been identified as ADORA1 agonists, and moreover, the latter have been detected in PVC samples by our group. As ADORA1 is an important therapeutic target in diseases, such as mood disorders, cardiac diseases, and stroke, disruption of ADORA1

signaling could have severe health effects. In total three plastic samples contain agonists for two GPCRs investigated in this thesis. MTNR1B and HTR2C were not activated by any plastic extracts, and thus, it was concluded that the plastic samples in this study did not contain agonists for these two receptors.

The results from the chemical analysis illustrated that potential GPCR agonists in active plastic samples can be narrowed down to a great extent. In this study, the lists of potential agonists obtained from non-target chemical analysis were reduced up to 86%. The cytotoxicity and PRESTO-Tango assay results in combination with the chemical analysis of this study contributes to reduce the knowledge gap regarding the chemical composition of plastics and points out that lists of potential GPCR agonists can be considerably reduced by excluding inactive FCCs through filtering steps.

The results from this study emphasize the importance of further research to identify FCCs that activate GPCRs. To further investigate the subject of this thesis, a bigger sample size and extraction of plastics in water would provide a more representative and realistic picture on GPCR activation by FCCs. In regard to the potential health effects of plastic chemical, several steps should be taken. First, humans are exposed to mostly mixtures of plastic polymers, and thus, mixture effects should be addressed. Risk assessments focuses on starting substances of plastics, and there are no regulations regarding mixture effects or NIAS despite the challenges of these being clear. Thus, FCMs contain numerous chemicals of unknow risks. To address the challenges regarding mixture effects and NIAS, and until these are better understood, clearer international regulations should be prioritized to ensure that FCAs does not include potentially harmful chemicals regardless of where they are produced. Further, transparency regarding plastics, whether being research, industry, or politics, are called for to approach plastic products that do not pose a risk to human health. By acknowledging the chemical complexity of plastics and welcoming transparency from all parts, further development of plastic product can improve the safety of this versatile material that on many levels has great benefits to humans.

Literature

ANDRADY, A. L. & NEAL, M. A. 2009. Applications and Societal Benefits of Plastics. *Philosophical Transactions of the Royal Society Biological Science,* 364**,** 1977-84.

AULD, D. S. & INGLESE, J. 2016. *Interferences with Luciferase Reporter Enzymes* [Online]. Available: https://www.ncbi.nlm.nih.gov/books/NBK374281/ [Accessed November 2022].

BARALIC, K., DJORDJEVIC, A. B., ŽIVANCEVIC, K., ANTONIJEVIC, E., MILENAANĐELKOVIC, DRAGANAJAVORAC, MARIJANACURCIC, ZORICABULAT, BILJANAANTONIJEVIC & ĐUKIC-COSIC, D. 2020. Toxic Effects of the Mixture of Phthalates and Bisphenol A—Subacute Oral Toxicity Study in Wistar Rats. *International Journal of Environmental Research and Public Health,* 17.

BEJGARN, S., MACLEOD, M., BOGDAL, C. & BREITHOLTZ, M. 2015. Toxicity of Leachate from Weathering Plastics: An Exploratory Screening Study with *Nitocra spinipes. Chemosphere,* 132.

BHALLA, M., HUI YEOH, J., LAMNECK, C., HERRING, S. E., TCHALLA, E. Y. I., HEINZINGER, L. R., LEONG, J. M. & BOU GHANEM, E. N. 2020. A1 Adenosine Receptor Signaling Reduces Streptococcus Pneumoniae Adherence to Pulmonary Epithelial Cells by Targeting Expression of Platelet-activating Factor Receptor. *Cellular Microbiology,* 22**,** e13141.

BIRMINGHAM, A., SELFORS, L. M., FORSTER, T., WROBEL, D., KENNEDY, C. J., SHANKS, E., SANTOYO-LOPEZ, J., DUNICAN, D. J., LONG, A., KELLEHER, D., SMITH, Q., BEIJERSBERGEN, R. L., GHAZAL, P. & SHAMU, C. E. 2009. Statistical Methods for Analysis of High-Throughput RNA Interference Screens. *Nat Methods,* 6**,** 569-575.

BJARNADÓTTIR, T. K., GLORIAM, D. E., HELLSTRAND, S. H., KRISTIANSSON, H., FREDRIKSSON, R. & SCHIÖTH, H. B. 2006. Comprehensive Repertoire and Phylogenetic Analysis of the G protein-coupled Receptors in Human and Mouse. *Genomics,* 88**,** 263-273.

BOREA, P. A., VARANI, K., GESSI, S., MERIGHI, S. & VINCENZI, F. 2018. *The Adenosine Receptors,* Cham, Springer International Publishing : Imprint : Humana.

CASTRO, B., SÁNCHEZ, P., MIRANDA, M. T., TORRES, J. M. & ORTEGA, E. 2015. Identification of Dopamine- and Derotonin-related Genes Modulated by Bisphenol A in the Prefrontal Cortex of Male Rats. *Chemosphere,* 139**,** 235-239.

CHEN, J., ALMO, S. C. & WU, Y. 2017. General Principles of Binding between Cell Surface Receptors and Multi-specific Ligands: A Computational Study. *PLoS Computational Biology,* 13**,** e1005805.

CHEN, W., GONG, Y., MCKIE, M., ALMUHTARAM, H., SUN, J., BARRETT, H., YANG, D., WU, M., ANDREWS, R. C. & PENG, H. 2022. Defining the Chemical Additives Driving In Vitro Toxicities of Plastics. *Environmental Science & Technology,* 56**,** 14627-14639.

CONOVER, W. J. 1999. *Practical Nonparametric Statistics*, John Wiley & Sons, Inc.

COUSSENS, N. P., AULD, D., ROBY, P., WALSH, J., BAELL, J. B., KALES, S., HADIAN, K. & DAHLIN, J. L. 2004. *The Assay Guidance Manual*, National Center for Advancing Translational Sciences.

DAHLIN, J. L., BAELL, J. & WALTERS, M. A. 2015. Assay Interference by Chemical Reactivity. *Assay Guidance Manual*.

DARBRE, P. D. 2020. Chemical Components of Plastics as Endocrine Disruptors: Overview and Commentary. *Birth Defects Research,* 112**,** 1300-1307.

DE ABREU COSTA, L., HENRIQUE FERNANDES OTTONI, M., DOS SANTOS, M. G., MEIRELES, A. B., GOMES DE ALMEIDA, V., DE FÁTIMA PEREIRA, W., ALVES DE AVELAR-FREITAS, B. & EUSTÁQUIO ALVIM BRITO-MELO, G. 2017. Dimethyl Sulfoxide (DMSO) Decreases Cell

Proliferation and TNF-α, IFN-γ, and IL-2 Cytokines Production in Cultures of Peripheral Blood Lymphocytes. *Molecules,* 22.

DESIMINE, V. L., MCCRINK, K. A., PARKER, B. M., WERTZ, S. L., MANING, J. & LYMPEROPOULOS, A. 2018. Chapter Two - Biased Agonism/Antagonism of Cardiovascular GPCRs for Heart Failure Therapy. *In:* SHUKLA, A. K. (ed.) *International Review of Cell and Molecular Biology.* Academic Press.

DIAMANTI-KANDARAKIS, E., BOURGUIGNON, J.-P., GIUDICE, L. C., RUSS HAUSER, PRINS, G. S., SOTO, A. M., ZOELLER, R. T. & GORE, A. C. 2009. Endocrine-Disrupting Chemicals: An Endocrine Society Scientific Statement. *Endocrine reviews,* 30**,** 293-342.

DOGRA, S., SONA, C., KUMAR, A. & YADAV, P. N. 2016. Tango Assay for Ligand-induced GPCR - β-arrestin2 Interaction: Application in Drug Discovery. *Methods in Cell Biology,* 132.

DU, X., LU, D., DAHARSH, E. D., YAO, A., DEWOODY, R. & YAO, J.-A. 2006. Dimethyl Sulfoxide Effects on hERG Channels Expressed in HEK293 Cells. *Journal of Pharmacological and Toxicological Methods,* 54**,** 164-172.

DUBOCOVICH, M. L. 2007. Melatonin Receptors: Role on Sleep and Circadian Rhythm Regulation. *Sleep Medicine,* 8**,** 34-42.

DUBOCOVICH, M. L., MASANA, M. I., IACOB, S. & SAURI, D. M. 1997. Melatonin Receptor Antagonists that Differentiate between the Human Mel1a and Mel1b Recombinant Subtypes are used to Assess the Pharmacological Profile of the Rabbit Retina ML1 Presynaptic Heteroreceptor. *Naunyn-Schmiedeberg's Archives of Pharmacology,* 355**,** 365-75.

ENVIRONMENTAL PROTECTION AGENCY. 2022. *CompTox Chemicals Dashboard: Assay Endpoints List* [Online]. Available: https://comptox.epa.gov/dashboard/assay-endpoints/ [Accessed November 2022].

FELSING, D. E., ANASTASIO, N. C., MISZKIEL, J. M., GILBERTSON, S. R., ALLEN, J. A. & CUNNINGHAM, K. A. 2018. Biophysical Validation of Serotonin 5-HT2A and 5-HT2C Receptor Interaction. *PLoS ONE,* 13.

FOSTER, R. G. 2021. Melatonin. *Current Biology,* 31**,** R1449-R1466.

GAO, N., HU, R., HUANG, Y., DAO, L., ZHANG, C., LIU, Y., WU, L., WANG, X., YIN, W., GORE, A. C. & SUN, Z. 2018. Specific Effects of Prenatal DEHP Exposure on Neuroendocrine Gene Expression in the Developing Hypothalamus of Male Rats. *Archives of Toxicology,* 92**,** 501-512.

GLATFELTER, G. C., JONES, A. J., RAJNARAYANAN, R. V. & DUBOCOVICH, M. L. 2021. Pharmacological Actions of Carbamate Insecticides at Mammalian Melatonin Receptors. *The Journal of Pharmacology and Experimental Therapeutics,* 376**,** 306-321.

GROB, K., BIEDERMANN, M., SCHERBAUM, E., ROTH, M. & RIEGER, K. 2006. Food Contamination with Organic Materials in Perspective: Packaging Materials as the Largest and Least Controlled Source? A View Focusing on the European Situation. *Critical Reviews in Food Science and Nutrition,* 46**,** 529-535.

GROH, K. J., BACKHAUS, T., CARNEY-ALMROTH, B., GEUEKE, B., INOSTROZA, P. A., LENNQUIST, A., LESLIE, H. A., MAFFINI, M., SLUNGE, D., TRASANDE, L., WARHURST, A. M. & MUNCKE, J. 2019. Overview of Known Plastic Packaging-associated Chemicals and heir Hazards. *Science of The Total Environment,* 651**,** 3253-3268.

HAHLADAKIS, J. N., VELIS, C. A., WEBER, R., IACOVIDOU, E. & PURNELL, P. 2018. An Overview of Chemical Additives Present in Plastics: Migration, Release, Fate and Environmental Impact during their Use, Disposal and Recycling. *Journal of Hazardous Materials,* 344**,** 179-199.

HANLON, C. D. & ANDREW, D. J. 2015. Outside-in Signaling – A Brief Review of GPCR Signaling with a Focus on the Drosophila GPCR Family. *The Company of Biologists,* 128**,** 3533-3542.

HARDELAND, R. 2012a. Melatonin in Aging and Disease - Multiple Consequences of Reduced Secretion, Options and Limits of Treatment. *Aging and Disease,* 3**,** 194-225.

HARDELAND, R. 2012b. Neurobiology, Pathophysiology, and Treatment of Melatonin Deficiency and Dysfunction. *The Scientific World Journal*.

HARDELAND, R., PANDI-PERUMAL, S. R. & CARDINALI, D. P. 2006. Melatonin. *The International Journal of Biochemistry & Cell Biology,* 38**,** 313-316.

HAUSER, A. S., ATTWOOD, M. M., RASK-ANDERSEN, M., SCHIÖTH, H. B. & GLORIAM, D. E. 2017. Trends in GPCR Drug Discovery: New Agents, Targets and Indications. *Nature Reviews Drug Discovery,* 16**,** 829-842.

HEITZLER, D., CRÉPIEUX, P., POUPON, A., CLÉMENT, F., FAGES, F. & REITER, E. 2009. Towards a Systems Biology Approach of G Protein-Coupled Receptor Signalling: Challenges and Expectations. *C. R. Biologies,* 332**,** 947-957.

HUANG, M., HUANG, M., LI, X., LIU, S., FU, L., JIANG, X. & YANG, M. 2021. Bisphenol A Induces Apoptosis Through GPER-dependent Activation of the ROS/Ca2+-ASK1-JNK Pathway in Human Granulosa Cell Line KGN. *Ecotoxicology and Environmental Safety,* 208**,** 111429.

JACOBSON, K. A. & GAO, Z.-G. 2006. Adenosine Receptors as Therapeutic Targets. *Nature Reviews Drug Discovery,* 5.

JANOWSKY, A., ESHLEMAN, A. J., JOHNSON, R. A., WOLFRUM, K. M., HINRICHS, D. J., YANG, J., ZABRISKIE, T. M., SMILKSTEIN, M. J. & RISCOE, M. K. 2014. Mefloquine and Psychotomimetics Share Neurotransmitter Receptor and tTansporter Interactions In Vitro. *Psychopharmacology (Berl),* 231**,** 2771-83.

JUREWICZ, J. & HANKE, W. 2011. Exposure to Phthalates: Reproductive Outcome and Children Health. A Review of Epidemiological Studies. *International Journal of Occupational Medicine and Environmental Health,* 24**,** 115-41.

KIM, T. K. & EBERWINE, J. H. 2010. Mammalian Cell Transfection: The Present and the Future. *Analytical and Bioanalytical Chemistry,* 397**,** 3173-8.

KOLB, P., KENAKIN, T., ALEXANDER, S. P. H., BERMUDEZ, M., BOHN, L. M., BREINHOLT, C. S., BOUVIER, M., HILL, S. J., KOSTENIS, E., MARTEMYANOV, K. A., NEUBIG, R. R., ONARAN, H. O., RAJAGOPAL, S., ROTH, B. L., SELENT, J., SHUKLA, A. K., SOMMER, M. E. & GLORIAM, D. E. 2022. Community Guidelines for GPCR Ligand Bias: IUPHAR Review 32. *British Journal of Pharmacology,* 179**,** 3651-3674.

KORTENKAMP, A. & FAUST, M. 2018. Regulate to Reduce Chemical Mixture Risk. *Science,* 361**,** 224-226.

KORTENKAMP, A., FAUST, M., SCHOLZE, M. & BACKHAUS, T. 2007. Low-Level Exposure to Multiple Chemicals: Reason for Human Health Concerns? *Environmental Health Perspectives,* 115**,** 106-114.

KROEZE, W. K., SASSANO, M. F., HUANG, X.-P., LANSU, K., MCCORVY, J. D., GIGUÈRE, P. M., SCIAKY, N. & ROTH, B. L. 2015. PRESTO-Tango as an Open-Source Resource for Interrogation of the Druggable Human GPCRome. *Nature Structural & Molecular Biology,* 22**,** 362-369.

LAUDON, M. & FRYDMAN-MAROM, A. 2014. Therapeutic Effects of Melatonin Receptor Agonists on Sleep and Comorbid Disorders. *International Journal of Molecular Sciences,* 15**,** 15924-50.

LAYLAND, J., CARRICK, D., LEE, M., OLDROYD, K. & BERRY, C. 2014. Adenosine. *JACC. Cardiovascular Interventions,* 7**,** 581-591.

LI, H.-X., GETZINGER, G. J., FERGUSON, P. L., ORIHUELA, B., ZHU, M. & RITTSCHOF, D. 2016. Effects of Toxic Leachate from Commercial Plastics on Larval Survival and Settlement of the Barnacle *Amphibalanus Amphitrite. Environmental Science & Technology,* 50**,** 924-931.

LITHNER, D., DAMBERG, J., DAVE, G. & LARSSON, K. 2009. Leachates from Plastic Consumer Products–Screening for Toxicity with *Daphnia Magna*. *Chemosphere,* 74**,** 1195-1200.

LITHNER, D., LARSSON, Å. & DAVE, G. 2011. Environmental and Health Hazard Ranking and Assessment of Plastic Polymers Based on Chemical Composition. *Science of The Total Environment,* 409**,** 3309-3324.

MAIN, K. M., MORTENSEN, G. K., KALEVA, M. M., BOISEN, K. A., DAMGAARD, I. N., CHELLAKOOTY, M., SCHMIDT, I. M., SUOMI, A. M., VIRTANEN, H. E., PETERSEN, D. V., ANDERSSON, A. M., TOPPARI, J. & SKAKKEBAEK, N. E. 2006. Human Breast Milk Contamination with Phthalates and Alterations of Endogenous Reproductive Hormones in Infants Three Months of Age. *Environmental Health Perspectives,* 114**,** 270-6.

MANSOURY, M., HAMED, M., KARMUSTAJI, R., HANNAN, F. A. & SAFRANY, S. T. 2021. The Edge Effect: A Global Problem. The Trouble with Culturing Cells in 96-well Plates. *Biochemistry and Biophysics Reports,* 26.

MCPARTLAND, M., STEVENS, S., VARDEBERG, I. G., VÖLKER, J. & WAGNER, M. 2022. Chemicals in Plastic Food Packaging Activate G protein-coupled Receptors. *In manuscript*.

MIRICK, D. K. & DAVIS, S. 2008. Melatonin as a Biomarker of Circadian Dysregulation. *Cancer Epidemiol Biomarkers Prev,* 17**,** 3306-3313.

MOON, M. K. 2019. Concern about the Safety of Bisphenol A Substitutes. *Diabetes & Metabolism Journal,* 43**,** 46-48.

MUNCKE, J., ANDERSSON, A., BACKHAUS, T., BOUCHER, J. M., ALMROTH, B. C., CASTILLO, A. C., CHEVRIER, J., DEMENEIX, B. A., EMMANUEL, J. A., FINI, J., GEE, D., GEUEKE, B., GROH, K., HEINDEL, J. J., HOULIHAN, J., KASSOTIS, C. D., KWIATKOWSKI, C. F., LEFFERT, L. Y., MAFFINI, M. V., MARTIN, O. V., MYERS, J. P., NADAL, A., NERIN, C., VANDENBERG, L. N., WAGNER, M., WU, C., ZOELLER, R. T. & SCHERINGER, M. 2020. Impacts of Food Contact Chemicals on Human Health: A Consensus Statement. *Environmental Health,* 19.

MUNCKE, J., BACKHAUS, T., GEUEKE, B., MAFFINI, M. V., MARTIN, O. V., MYERS, J. P., SOTO, A. M., TRASANDE, L., TRIER, X. & SCHERINGER, M. 2017. Scientific Challenges in the Risk Assessment of Food Contact Materials. *Environmental Health Perspectives,* 129.

NAKAMURA, K., ITOH, K., YOSHIMOTO, K., SUGIMOTO, T. & FUSHIKI, S. 2010. Prenatal and lactational exposure to low-doses of bisphenol A alters brain monoamine concentration in adult mice. *Neuroscience Letters,* 484**,** 66-70.

PLASTICSEUROPE 2021. Plastics - the Facts 2021.

POPOVSKA-GOREVSKI, M., DUBOCOVICH, M. L. & RAJNARAYANAN, R. V. 2017. Carbamate Insecticides Target Human Melatonin Receptors. *Chemical Research in Toxicology,* 30**,** 574-582.

PROMEGA 2010. Wizard® Plus Midipreps DNA Purification System.

PUPO, M., PISANO, A., LAPPANO, R., SANTOLLA, M. F., DE FRANCESCO, E. M., ABONANTE, S., ROSANO, C. & MAGGIOLINI, M. 2012. Bisphenol A Induces Gene Expression Changes and Proliferative Effects through GPER in Breast Cancer Cells and Cancer-Associated Fibroblasts. *Environmental Health Perspectives,* 120**,** 1177-1182.

ROSENBAUM, D. M., RASMUSSEN, S. G. F. & KOBILKA, B. K. 2009. The Structure and Function of G-protein-coupled Receptors. *Nature,* 459.

ROT, B. L. & KROEZE, W. K. 2015. Integrated Approaches for Genome-wide Interrogation of the Druggable Non-olfactory G Protein-coupled Receptor Superfamily. *Journal of Biological Chemistry,* 290**,** 19471-19477.

SARKAR, P., MOZUMDER, S., BEJ, A., MUKHERJEE, S., SENGUPTA, J. & CHATTOPADHYAY, A. 2020. Structure, Dynamics and Lipid Interactions of Serotonin Receptors: Excitements and Challenges. *Biophysical Reviews,* 13**,** 101-122.

SCHNEIDER, J., KORSHUNOVA, K., MUSIANI, F., ALFONSO-PRIETO, M., GIORGETTI, A. & CARLONI, P. 2018. Predicting Ligand Binding Poses for Low-Resolution Membrane Protein Models: Perspectives from Multiscale Simulations. *Biochemical and Biophysical Research Communications,* 498.

SHARMA, H. S. 2004. *Influence of Serotonin on the Blood–Brain and the Blood–Spinal Cord Barriers,* Blood-Spinal Cord and Brain Barriers in Health and Disease.

SINGH, M., MCKENZIE, K. & MA, X. 2017. Effect of Dimethyl Sulfoxide on In Vitro Proliferation of Skin Fibroblast Cells. *Journal of Biotech Research,* 8**,** 78-82.

SKÅLAND, H. S. 2022. *Non-Target Analysis of Chemicals Extracted and Migrated from Plastic Food Contact Articles.* Norwegian University of Science and Technology.

SRIDHARAN, S., KUMAR, M., SAHA, M., KIRKHAM, M. B., SINGH, L. & BOLAN, N. S. 2022. The Polymers and their Additives in Particulate Plastics: What Makes them Hazardous to the Fauna? *Science of The Total Environment,* 824**,** 153828.

SRIRAM, K. & INSEL, P. A. 2018. G Protein-Coupled Receptors as Targets for Approved Drugs: How Many Targets and How Many Drugs? *Molecular Pharmacology,* 93**,** 251-258.

STIRLING, D. R., SWAIN-BOWDEN, M. J., LUCAS, A. M., CARPENTER, A. E., CIMINI, B. A. & GOODMAN, A. 2021. CellProfiler 4: Improvements in Speed, Utility and Usability. *BMC Bioinformatics,* 22.

STRANGE, P. G. 2008. Agonist Binding, Agonist Affinity and Agonist Efficacy at G protein-Coupled Receptors. *British Journal of Pharmacology,* 153**,** 1353-63.

SUM, C. S., MURPHY, B. J., LI, Z., WANG, T., ZHANG, L. & CVIJIC, M. E. 2019. *Pharmacological Characterization of GPCR Agonists, Antagonists, Allosteric Modulators and Biased Ligands from HTS Hits to Lead Optimization.* [Online]. Assay Guidance Manual [Internet]. Available: https://www.ncbi.nlm.nih.gov/books/NBK549462/ [Accessed].

THERMOFISHER SCIENTIFIC. 2022. *Factors Influencing Transfection Efficiency* [Online]. Available: https://www.thermofisher.com/no/en/home/references/gibco-cell-culture-basics/transfection-basics/factors-influencing-transfection-efficiency.html [Accessed November 2022].

TILLEY, D. G. 2012. G Protein-Dependent and G Protein-Independent Signaling Pathways and their Impact on Cardiac Function. *Circulation Research,* 109**,** 217-230.

VOM SAAL, F. S. & WELSHONS, W. V. 2006. Large Effects from Small Exposures. II. The Importance of Positive Controls in Low-Dose Research on Bisphenol A. *Environmental Research,* 100**,** 50-76.

VÖLKER, J., ASHCROFT, F., VEDØY, Å., ZIMMERMANN, L. & WAGNER, M. 2022. Adipogenic Activity of Chemicals Used in Plastic Consumer Products. *Environmental Science & Technology,* 56**,** 2487-2496.

WALDMAN, S. A. 2009. CHAPTER 5 - DRUG-RECEPTOR INTERACTIONS. *In:* WALDMAN, S. A., TERZIC, A., EGAN, L. J., ELGHOZI, J.-L., JAHANGIR, A., KANE, G. C., KRAFT, W. K., LEWIS, L. D., MORROW, J. D., ZINGMAN, L. V., ABERNETHY, D. R., ATKINSON, A. J., BENOWITZ, N. L., BRATER, D. C., GRAY, J., HONIG, P. K., KEARNS, G. L., LEVEY, B. A., SPIELBERG, S. P., WEINSHILBOUM, R. & WOOSLEY, R. L. (eds.) *Pharmacology and Therapeutics.* Philadelphia: W.B. Saunders.

WANG, J., GARERI, C. & ROCKMAN, H. A. 2018. G-Protein–Coupled Receptors in Heart Disease. *Circulation Research,* 123**,** 716-735.

WIESINGER, H., WANG, Z. & HELLWEG, S. 2021. Deep Dive into Plastic Monomers, Additives, and Processing Aids. *Environmental Science & Technology,* 55**,** 9339-9351.

WORLD HEALTH ORGANIZATION 2022. Dietary and Inhalation Exposure to Nano- and Microplastic Particles and the Potential Implications for Human Health. Geneva.

YOUNG, S. N. 2007. How to Increase Serotonin in the Human Brain without Drugs. *Journal of Psychiatry and Neuroscience,* 32**,** 394-399.

ZHANG, J.-H., CHUNG, T. D. Y. & OLDENBURG, K. R. 1999. A Simple Statistical Parameter for Use in Evaluation and Validation of High Throughput Screening Assays. *Journal of Biomolecular Screening,* 4.

ZHAO, J., DENG, Y., JIANG, Z. & QING, H. 2016. G Protein-Coupled Receptors (GPCRs) in Alzheimer's Disease: A Focus on BACE1 Related GPCRs. *Frontiers in Aging Neuroscience,* 8**,** 58.

ZIMMERMANN, L., BARTOSOVA, Z., BRAUN, K., OEHLMANN, J., VÖLKER, C. & WAGNER, M. 2021. Plastic Products Leach Chemicals That Induce In Vitro Toxicity under Realistic Use Conditions. *Environmental Science and Technology,* 55**,** 11814-11823.

ZIMMERMANN, L., DIERKES, G., TERNES, T. A., VÖLKER, C. & WAGNER, M. 2019. Benchmarking the in Vitro Toxicity and Chemical Composition of Plastic Consumer Products. *Environmental Science and Technology,* 53**,** 11467-11477.

ŻMUDZKA, E., SAŁACIAK, K., SAPA, J. & PYTKA, K. 2018. Serotonin Receptors in Depression and Anxiety: Insights from Animal Studies. *Life Science,* 210**,** 106-124.

APPENDIX A – Materials

Table A.1: List of materials used in this thesis, including producer/distributor and product number.

Material	Distributor	Product number
HTLA CELLS	Roth Lab PRESTO-Tango GPCR Kit	
Plasmid DNA	Addgene	Kit #1000000068
Dulbecco's Modified Eagle Medium (DMEM) – high glucose	Sigma-Aldrich	D6429
Fetal Bovine Serum (FBS)	Gibco	A4766801
Dialyzed Fetal Bovine Serum (dFBS)	ThermoFisher	A3382001
Penicillin/Streptomycin	VWR	L0022-100
Trypsin/EDTA	Sigma-Aldrich	59418C
Puromycin	Invivogen	Ant-pr-1
Hygomycin	Invivogen	Ant-hg-1
Ampicillin	Sigma-Aldrich	A1000000
Lipofectamine™ 3000 Transfection Reagent	ThermoFisher	L3000008
Opti-MEM™ Reduced Serum Medium	ThermoFisher	31985062
Poly-L-lysine Hydrobromide (PLL)	Sigma-Aldrich	P2636
D-luciferin, Monopotassium Salt	Pierce	88294
Adenosine 5'-Triphosphoric Acid Disodium Salt BioChemica	PanReac AppliChem	A1348,0005
DL-Dithiothreitol	Sigma-Aldrich	D0632
NucBlue™ Live ReadyProbes™ Reagent (Hoechst 33342)	Invitrogen	R37605
Wixard® *Plus* Midipreps DNA Purification System	Promega	A7640
Tricine	Sigma-Aldrich	T0377
EDTA	Bio-Rad	140930A
Magnesium Sulfate	Sigma-Aldrich	M2643
Trans-1,2-Diaminocyclohexane-N,N,N',N'-tetraacetic Acid Monohydrate	Sigma-Aldrich	32869
Magnesium Carbonate Hydroxide Pentahydrate	Alfa Aesar	A18070
Trizma® Base	Sigma-Aldrich	93350
Triton™ X-100	Sigma-Aldrich	X100
Glycerol	Promega	H5433
Tryptone	VWR	84610.0500

Yeast Extract	Sigma-Aldrich	Y1625
Sodium Phosohate Dibasic	Sigma-Aldrich	S5136
Potassium Phosphate Monobasic	Sigma-Aldrich	P5655
Sodium Chloride	Sigma-Aldrich	S6150
Potassium Chloride	Sigma-Aldrich	P9541
TRIS hydrochloride	Sigma-Aldrich	PHG0002

Table A.2: DMEM growth media content, 555 mL.

Reagent	Amount
Dulbecco's Modified Eagle Medium (DMEM)	500 mL
Fetal bovine serum (FBS)	50 mL
Penicillin streptomycin	5 mL

Table A.3: DMEM starving media content, 510 mL.

Reagent	Amount
Dulbecco's Modified Eagle Medium (DMEM)	500 mL
Dialyzed fetal bovine serum (dFBS)	5 mL
Penicillin streptomycin	5 mL

Table A.4: Phosphate-buffered saline (PBS) content, 1 L.

Reagent	Amount
Na_2HPO_4	1.42 g
KH_2PO_4	0.24 g
NaCl	8 g
KCl	0.2 g
Ultrapure H_2O (PURELAB flex, ELGA)	Adjust to 1 L

Table A.5: TE-buffer content, 100 mL.

Reagent	Volume	Final concentration
Tris-HCl (1 M, pH 8.0)	1 mL	10 mM
EDTA (0.5 M, pH 8.0)	0.2 mL	1 mM
Ultrapure H_2O (PURELAB flex, ELGA)	98.8 mL	

Table A.6: Liquid lysogeny broth (LB) media content, 800 mL.

Reagent	Amount
NaCl	8 g
Tryptone	8 g
Yeast extract	4 g
Ultrapure H_2O (PURELAB flex, ELGA)	Adjust to 800 mL

Table A.7: Cell lysis buffer content, 1 L.

Compound	Weight	Volume	Molecular weight	Molarity
Tris	3.0 g		121.1 g/mol	25 mM
DTT	0.31 g		154.2 g/mol	2,0 mM
CDTA	0.73 g		364.35 g/mol	2,0 mM
Glycerol		100 ml		10%
Triton®X-100		10 ml		1%

Table A.8: Luminescence Mix content, 1 L.

Compound	Weight	Molecular weight	Molarity
Tricine	3.580 g	179.2 g/mol	20.0 mM
$(MgCO_3)_4$ Mg $(OH)_2$ * 5 H2O	0.520 g	485.69 g/mol	1.07 mM
$MgSO_4$ * 7 H_2O	0.658 g	246.48 g/mol	2.67 mM
EDTA	0.037 g	372.23 g/mol	0.10 mM
DTT	0.231 g	154.2 g/mol	1.5 mM
D-Luciferine	0.151 g	280.3 g/mol	539 µM
ATP	3.026 g	551.1 g/mol	5.49 mM

APPENDIX B – PRESTO-Tango procedure details

Table B.1: Procedure on mixing of DNA-lipid complex for transfecting HTLA cells with plasmid DNA.

Step	Placement and volume	Reagents	Action
1	In 1.5 µL microcentrifuge tube, for 384 wells.	1296 µL Opti-MEM. 50 µL LIPO3000.	Mix by vortexing well.
2	In each A-well of 96-well plate, for 32 wells.	108 µL Opti-MEM. 45 µL plasmid DNA. 4.5 µL P3000.	Mix with multichannel pipet (P/M setting).
3	In each A-well of 96-well plate from step 2.	115 µL of Opti-MEM/LIPO3000 mix from step 1.	Mix with multichannel pipet (P/M setting). Incubate for 15 min.
4	In each A well of 96-well plate from step 2 and 3.	96.5 µL Opti-MEM.	Mix with multichannel pipet (P/M setting).
5	In each well of the 384-well plate.	10 µL DNA-lipid complex from A wells from step 4.	Be sure to get the DNA-lipid complex on the cells.

Table B.2: Dilutions of the reference compounds used as reference compounds and of plastic extracts in the PRESTO-Tango assay.

Step	Reference compound (melatonin and LSD)	Reference compound (NECA)	Plastic chemicals	PUR (diluted)	Solvent control (DMSO)
A	1 µL melatonin/LSD 20 mM into 999 µL starving media	10 µL NECA 10 mM into 990 µL starving media	1.4 µL plastic chemical into 358.56 µL starving media.	0.72 µL plastic chemical into 719.28 µL starving media.	1.4 µL DMSO into 358.56 µL starving media.
B	60 µL from step A into 540 µL starving media.	60 µL from step A into 540 µL starving media.	180 µL from step A into 180 µL starving media.	360 µL from step A into 360 µL starving media.	180 µL from step A into 180 µL starving media.
C	60 µL from step B into 540 µL starving media.	60 µL from step B into 540 µL starving media.	180 µL from step B into 180 µL starving media.	360 µL from step B into 360 µL starving media.	180 µL from step B into 180 µL starving media.
D	60 µL from step C into 540 µL starving media.	60 µL from step C into 540 µL starving media.	180 µL from step C into 180 µL starving media.	360 µL from step C into 360 µL starving media.	360 µL starving media (negative control).
E	60 µL from step D into 540 µL starving media.	60 µL from step D into 540 µL starving media.	180 µL starving media (negative control).	360 µL from step D into 360 µL starving media.	360 µL starving media (negative control).
F	60 µL from step E into 540 µL starving media.	60 µL from step E into 540 µL starving media.	180 µL from step D into 180 µL starving media.	360 µL from step E into 360 µL starving media.	180 µL from step C into 180 µL starving media.
G	60 µL from step F into 540 µL starving media.	60 µL from step F into 540 µL starving media.	180 µL from step F into 180 µL starving media.	360 µL from step F into 360 µL starving media.	180 µL from step F into 180 µL starving media.

APPENDIX C – R packages

R packages used for interpretation and analysis in this thesis was:

- ‘ggpubr’
- ‘drc’
- ‘devtools’
- ‘tidyverse’
- ‘rstatix’
- ‘pheatmap’
- ‘dplyr’
- ‘RColorBrewer’

APPENDIX D - Positive control dose-response curve and plastic extract activation for each PRESTO-Tango assay

Explanation to abbreviations in Table D.1:

PE1 = ALL34

PE2 = ALL14

PE3 = ALL10

PP1 = ALL17

PP2 = ALL39b

PS1 = ALL33

PS2 = ALL41

PUR = ALL12

PVC1 = PVC29

PVC2 = PVC4

PVC3 = PVC26

Diverse polymer mix = ALLmix

PVC mix = PVCmix

Table D.1: Positive control concentration-response curve and plastic extract activation for each PRESTO-Tango assay.

Exp. Nr.	Receptor	PC concentration-response curve (x axis = fold activation)	Treatment concentration-response curve (x axis = normalized luminescence to the PC (% activation).
1	MTNR1A	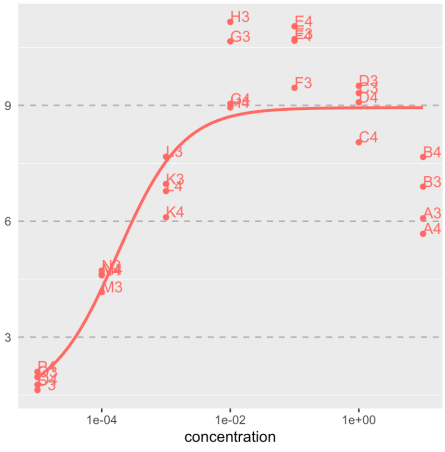	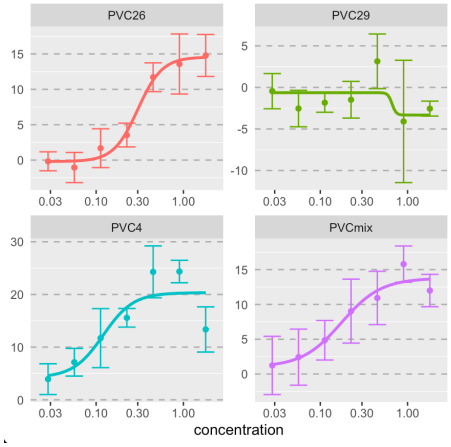

2 MTNR1A

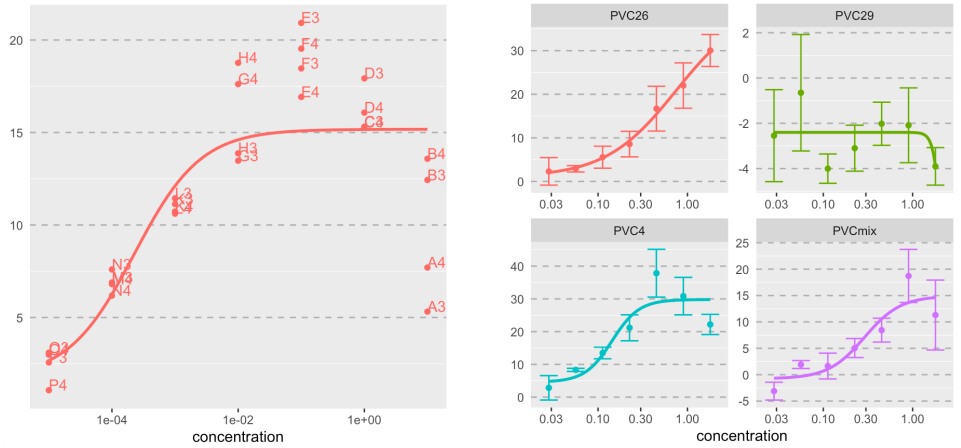

3 MTNR1A

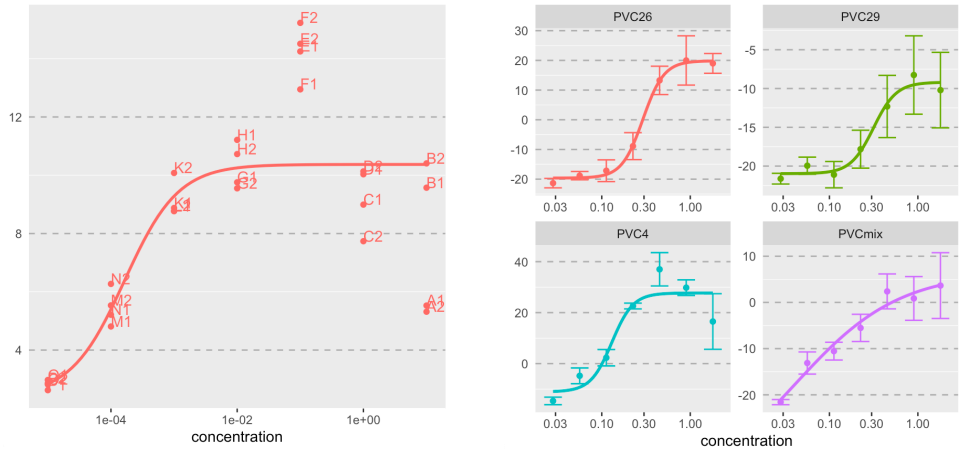

3 MTNR1B

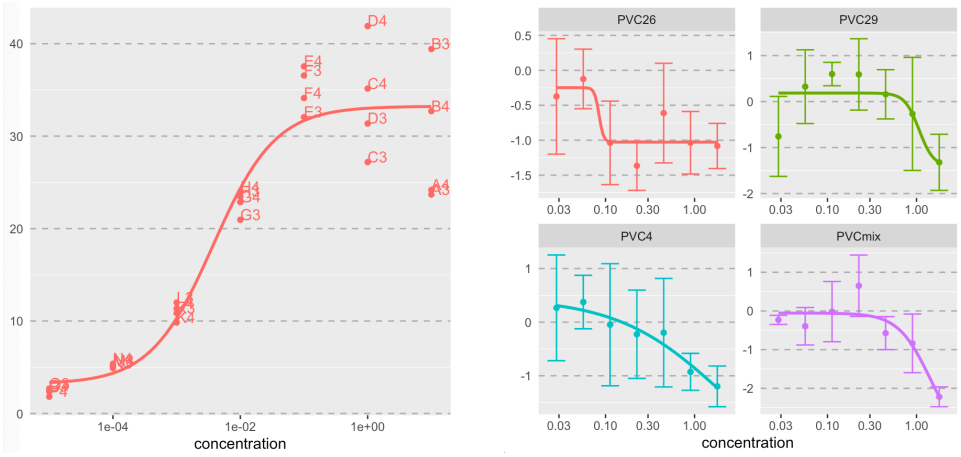

4 MTNR1A

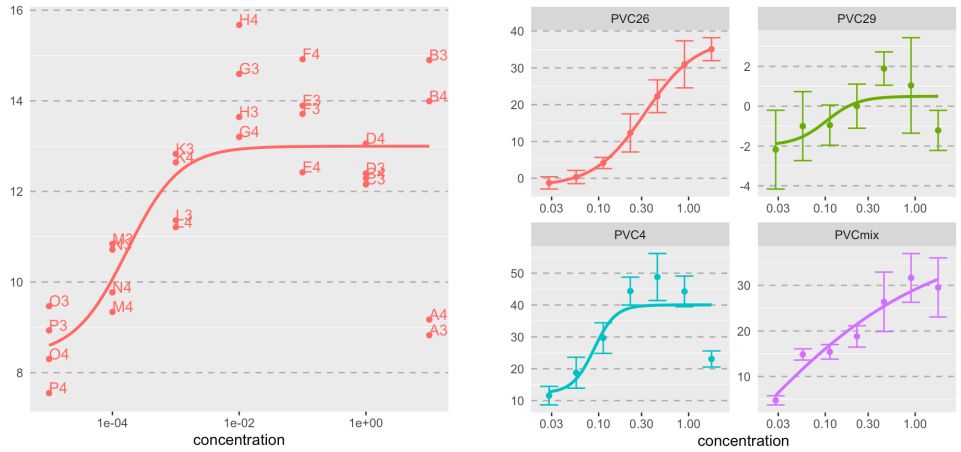

5 MTNR1B

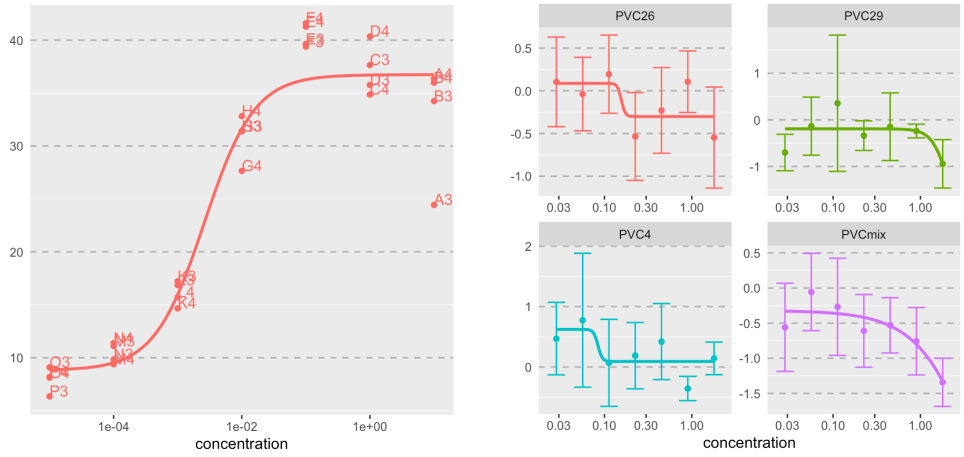

6 ADORA1

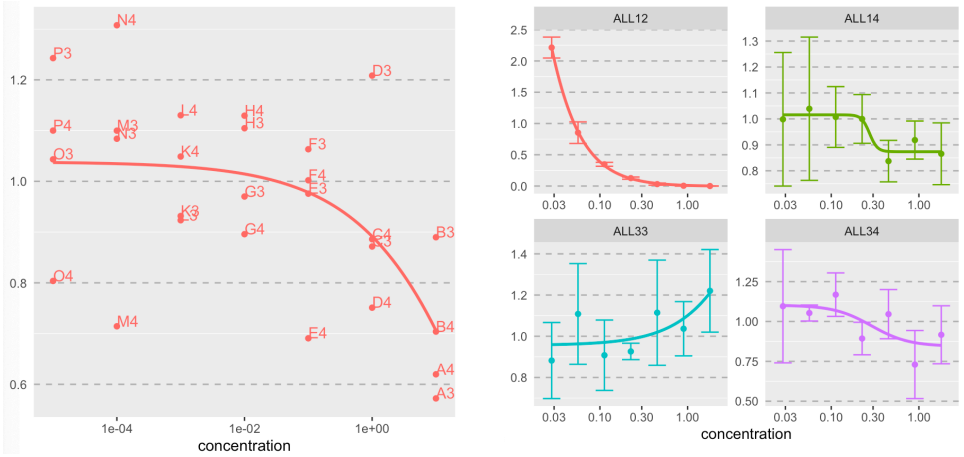

7 MTNR1B

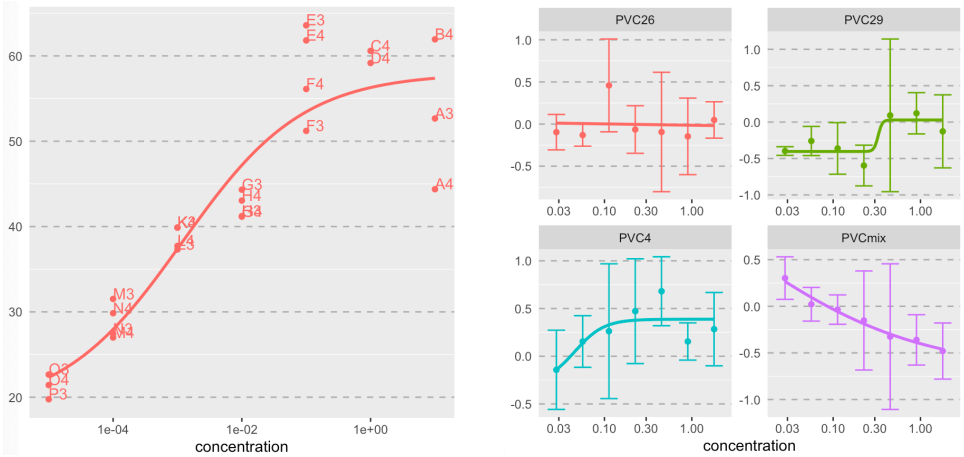

8 MTNR1A

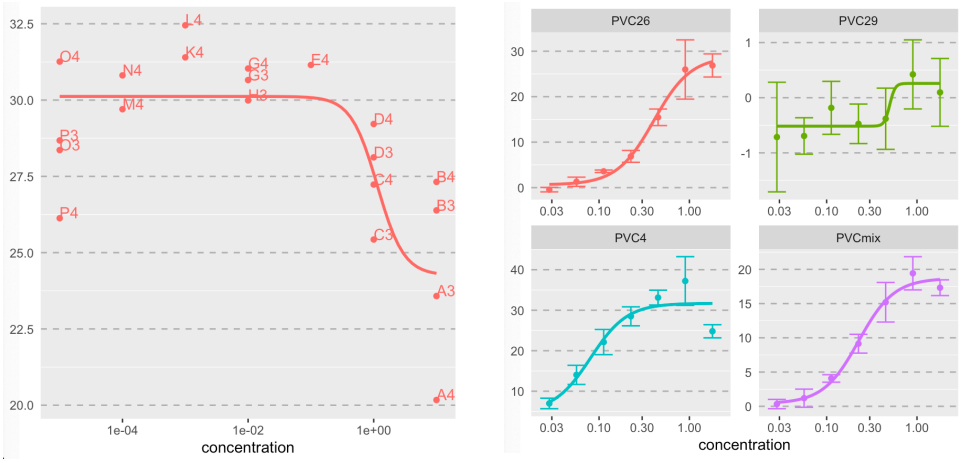

9 ADORA1

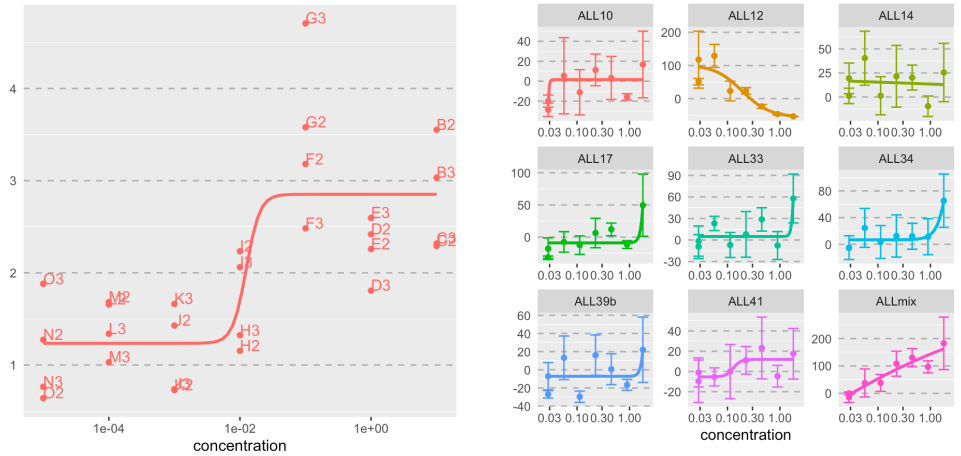

10 ADORA1

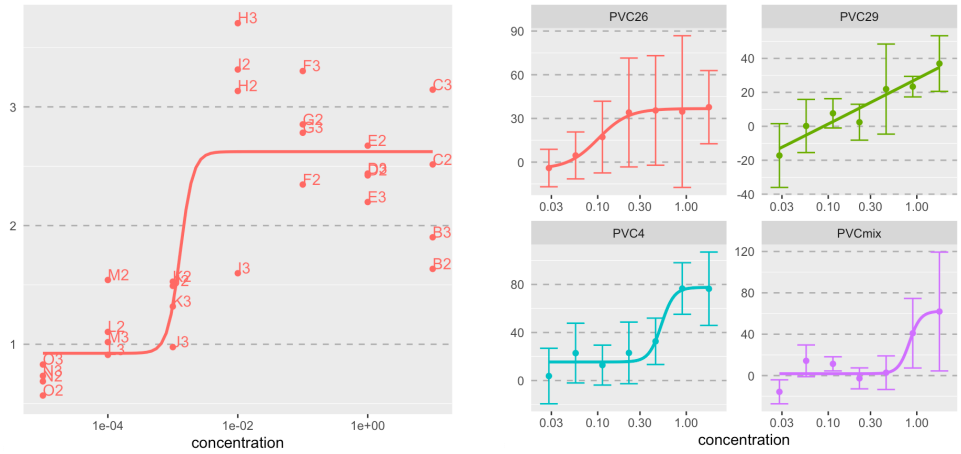

11 MTNR1A

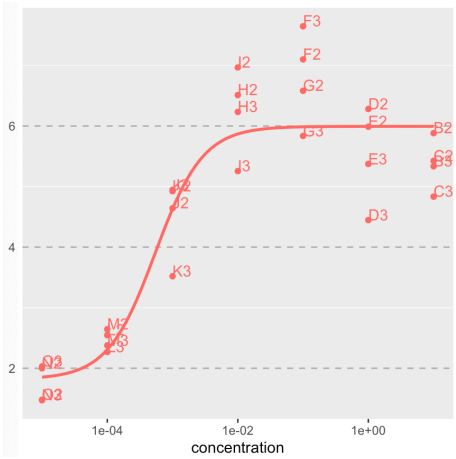

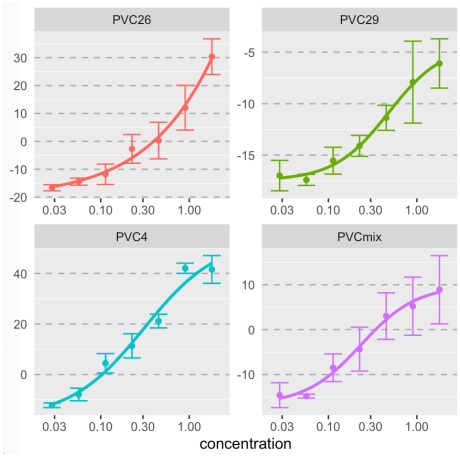

12 ADORA1

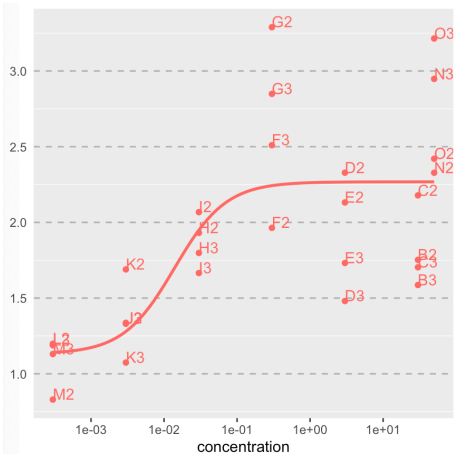

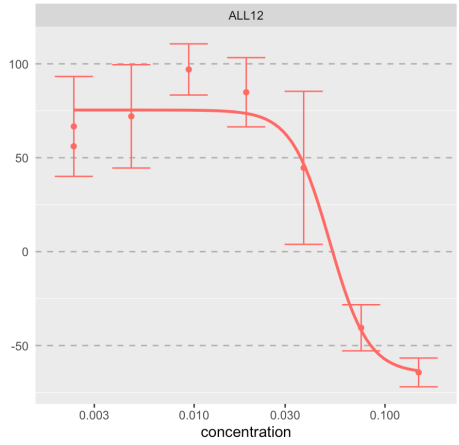

12 HTR2C

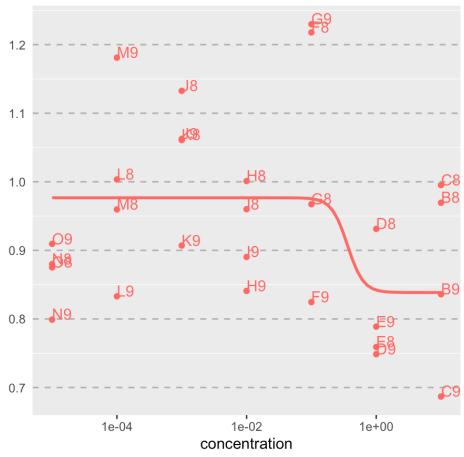

* No plastic extract treatment

12 HTR1A

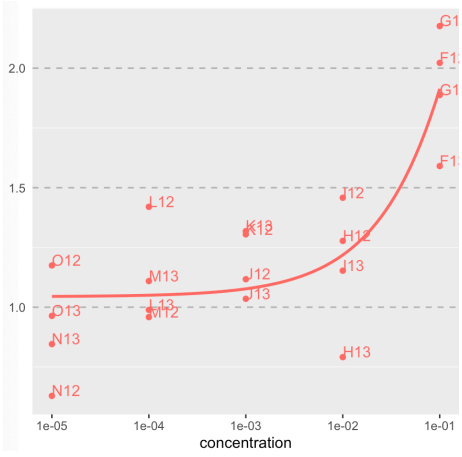

* No plastic extract treatment

13 MTNR1A

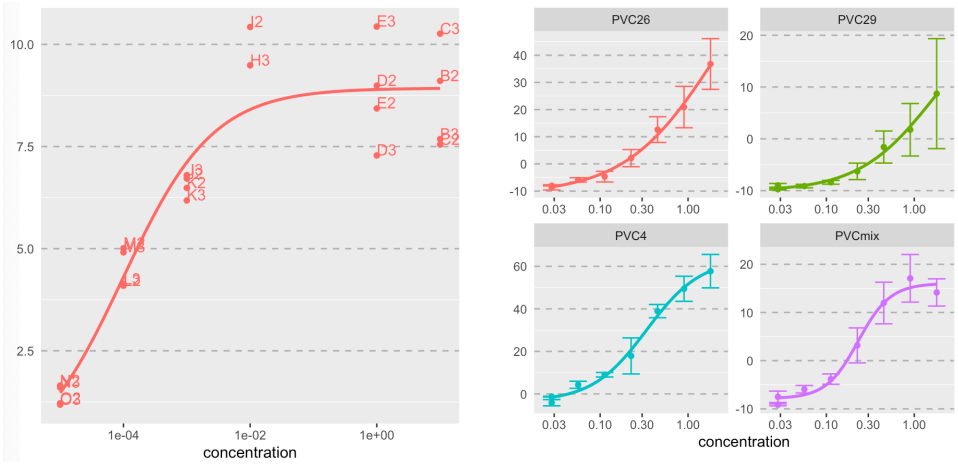

14 ADORA1

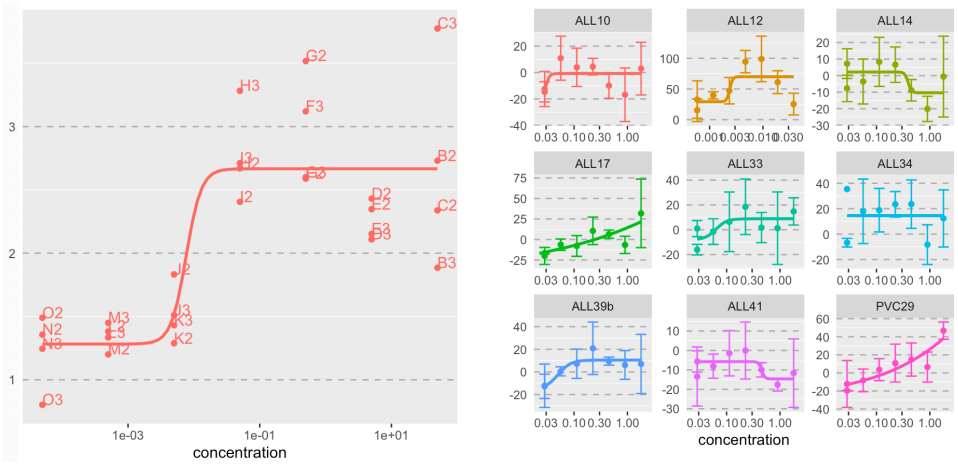

15 HTR1A

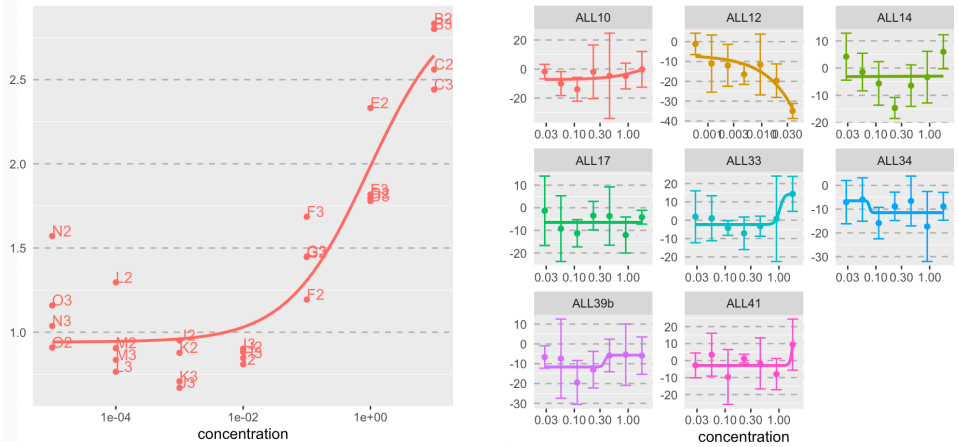

16 ADORA1

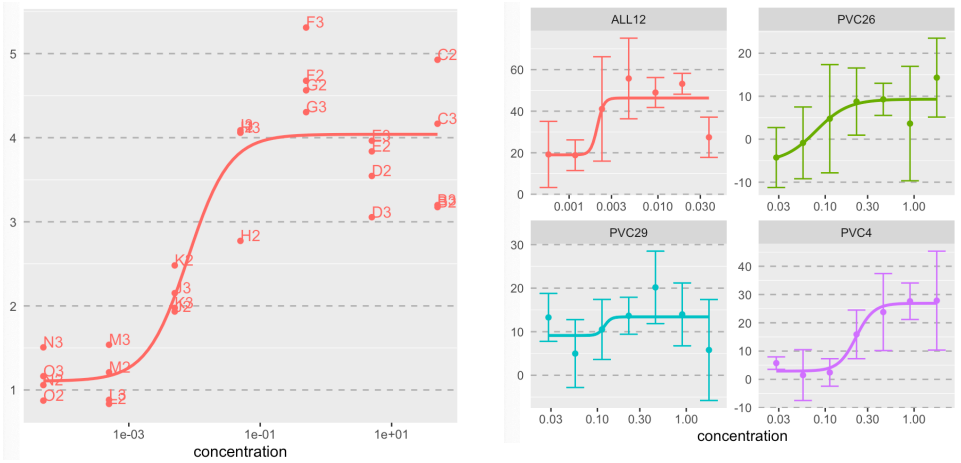

17 HTR1A

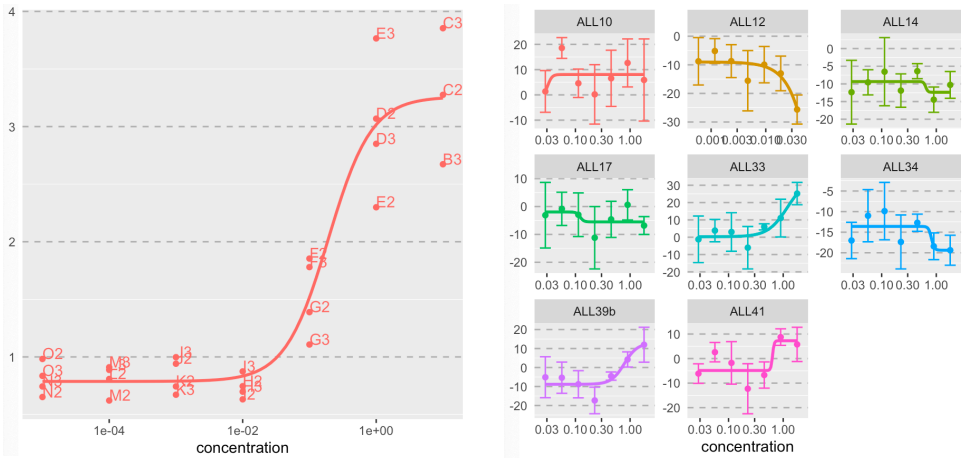

18 ADORA1

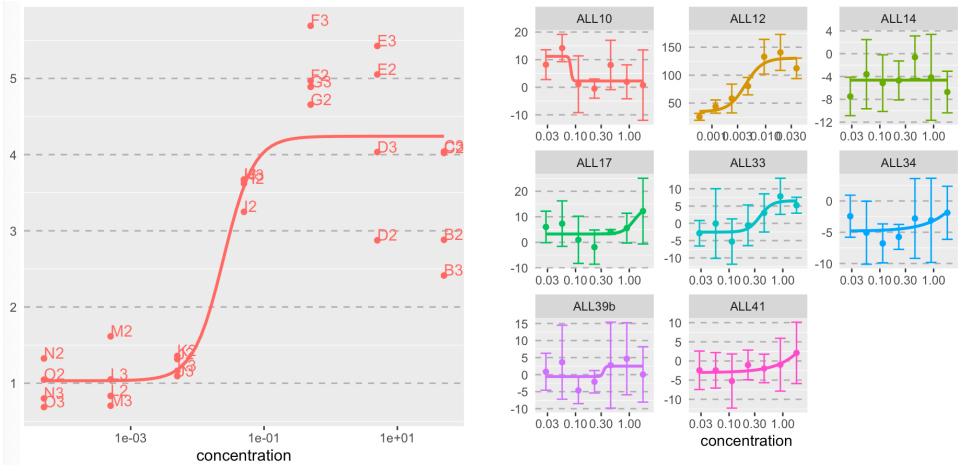

19 ADORA1

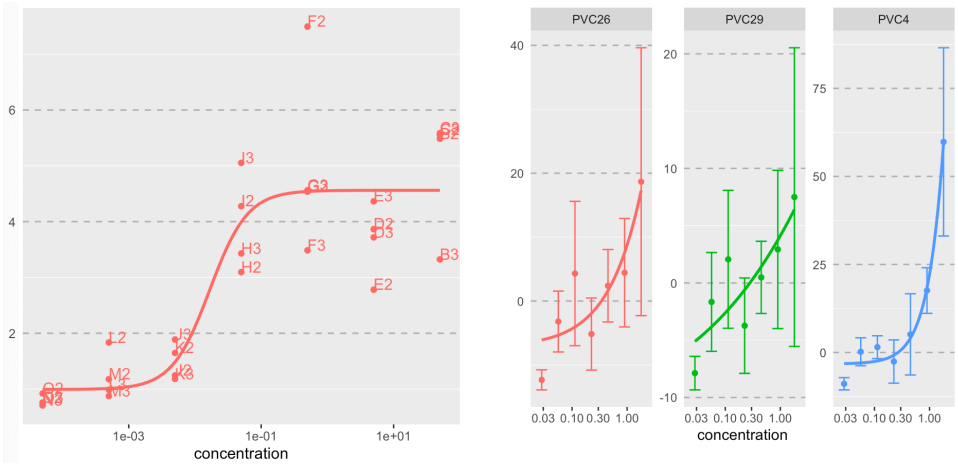

20 ADORA1

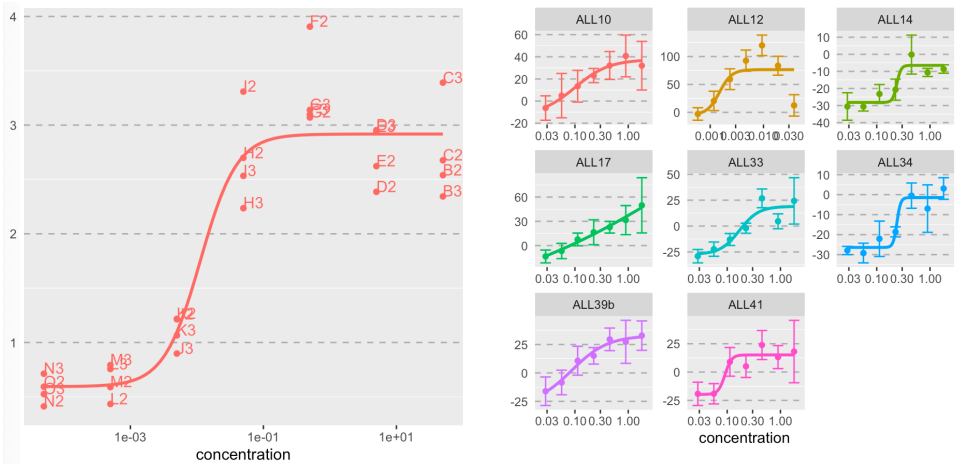

21 ADORA1

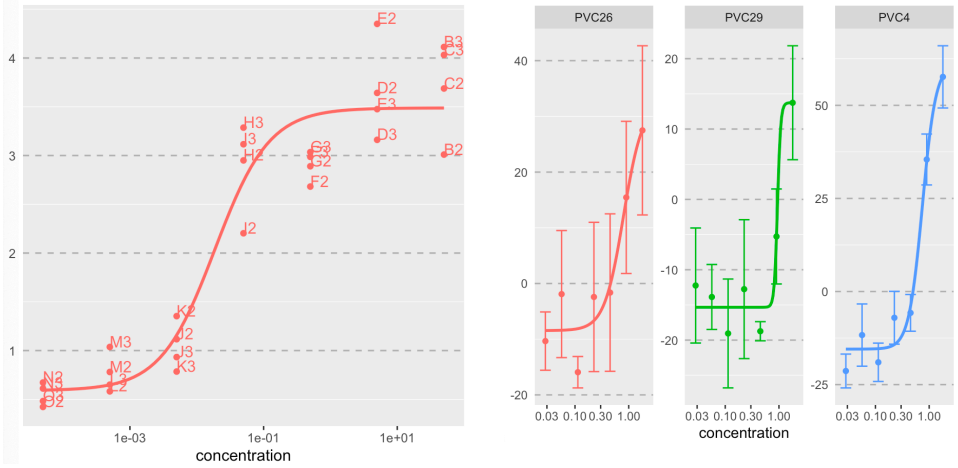

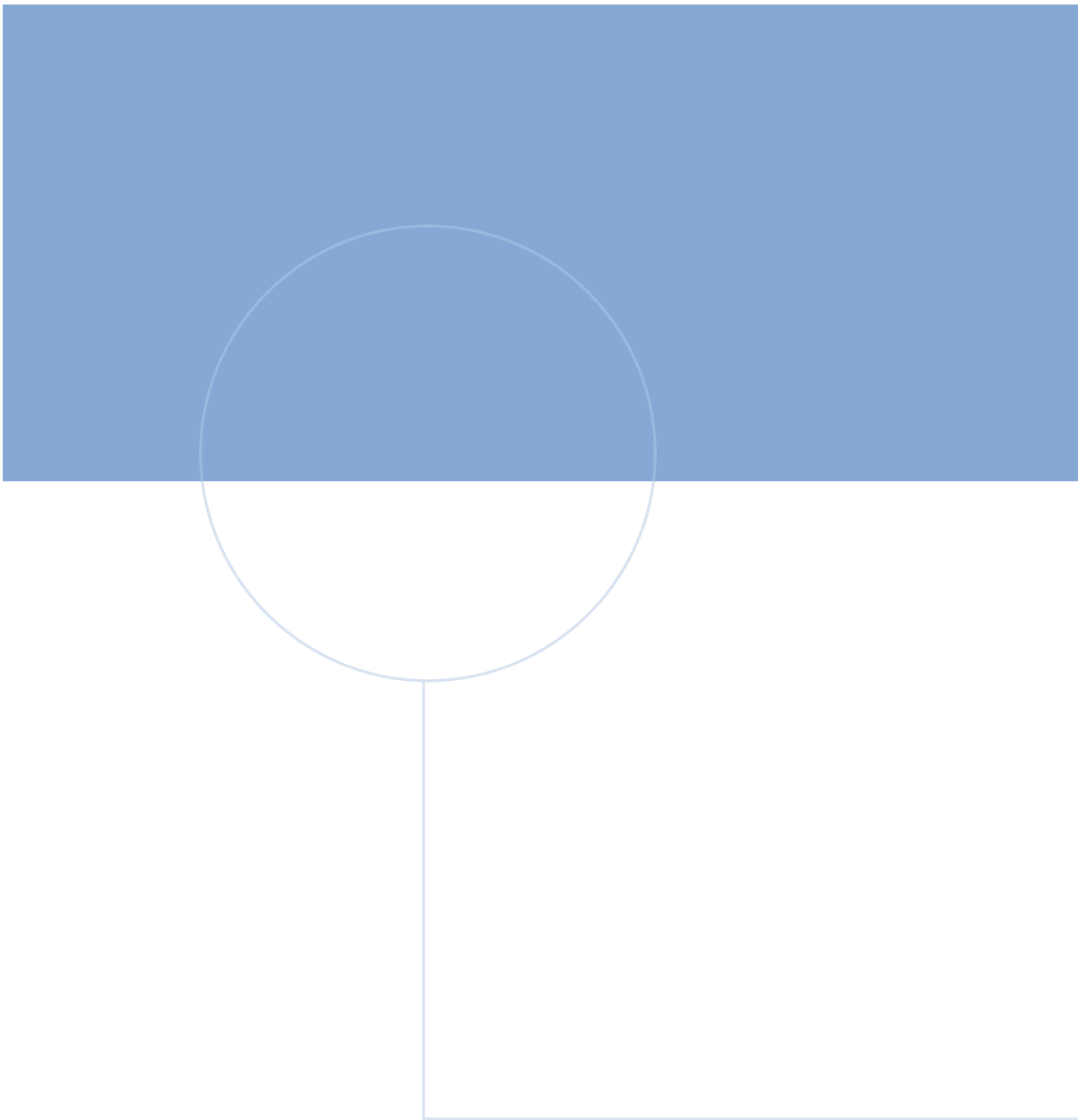

NTNU

Norwegian University of
Science and Technology